



Synthesis and in vitro antitumour activity of 4(R)-methyl-3-O-phosphonomethyl- α -L-threose nucleosides



Feng-Wu Liu^{a,*}, Shujie Ji^a, Yingying Gao^a, Yao Meng^a, Wenke Xu^a, Haixia Wang^a, Jing Yang^a, Hao Huang^a, Piet Herdewijn^b, Cong Wang^{a,**}

^a Key Laboratory of Advanced Drug Preparation Technologies, Ministry of Education of China, School of Pharmaceutical Sciences, Zhengzhou University, Zhengzhou, 450001, PR China

^b Medicinal Chemistry, Rega Institute for Medical Research, KU Leuven, Herestraat 49, 3000, Leuven, Belgium

ARTICLE INFO

Article history:

Received 3 January 2021

Received in revised form

16 April 2021

Accepted 27 April 2021

Available online 14 May 2021

Keywords:

α -L-threose nucleoside phosphonate analogs

D-xylose

Antitumour activity

Mechanistic investigations

ABSTRACT

A series of novel α -L-threose nucleoside phosphonate analogs, 4(R)-methyl-3-O-phosphonomethyl- α -L-threose nucleosides, were synthesized in multistep sequences starting from D-xylose. The synthetic sequence consisted of the following key stages: (i) the multistep synthesis of 1,2-O-isopropylidene-4(R)-methyl-3-O-phosphonomethyl-L-threose, (ii) the transformation of 1,2-O-isopropylidene sugar into suitable 1,2-di-O-acyl L-threose precursor, and (iii) the construction of target α -L-threose nucleoside phosphonate analogs by Vorbrüggen glycosidation reaction, deprotection of acyl group, and hydrolysis of diethyl group on phosphonate. The target nucleoside phosphonates were evaluated for their antitumour activities in cell culture-based assays. Compound **8g**, 2-fluoroadenosine phosphonate, showed remarkable activity against human breast cancer cell lines (MCF-7 and MDA-MB-231) with IC₅₀ values of 0.476 and 0.391 μ M, corresponding to 41- and 47-fold higher potency than the reference compound 5-FU, respectively. Subsequent investigations found that the compound **8g** can inhibit the proliferation of breast cancer cells and cell cloning. The mechanistic studies indicated that compound **8g** could cause DNA damage to breast cancer cells through the ATM-Chk1/Chk2-cdc25c pathway, leading to blockage of the G2/M phase cycle of breast cancer cells, which ultimately led to apoptosis. Moreover, **8g** could inhibit the PI3K/AKT signaling pathway and induce apoptosis. These results indicate that compound **8g** holds promising potential as an antitumour agent.

© 2021 Elsevier Masson SAS. All rights reserved.

1. Introduction

Modified nucleoside analogs have occupied an important position within medicine for the treatment of viral disease and cancer for decades. Development of novel nucleoside drugs mainly focused on chemical modification of both sugar and nucleobase moiety. Nucleosides modified at the base or sugar moiety generally are prodrugs, which enter cells and are anabolized by nucleoside kinases to their mononucleotides, then to the bioactive 5-triphosphates via two subsequent phosphorylations. The triphosphate metabolites are incorporated into DNA during replication, leading to termination of DNA chain elongation [1].

One main challenge encountered in the development of nucleoside drugs is their limited capacity to undergo in vivo stepwise phosphorylation to their biologically active nucleoside triphosphate to express their therapeutic effect [2]. Within the nucleoside analog phosphorylation process, the first phosphorylation to nucleoside monophosphate is often the rate-limiting step [3]. Furthermore the nucleoside monophosphate is susceptible to hydrolysis by phosphatase leading to free nucleoside analog, which results in the lower efficiency of first phosphorylation. In order to address the problem, medicinal chemists make efforts to prepare nucleoside phosphonate. As isosteric analog of a nucleoside monophosphate, phosphonate has the advantage over its phosphate counterpart due to its P–C bond being stable to phosphatase hydrolysis and phosphonate being readily phosphorylated further by cellular kinases [4]. Nucleoside phosphonates are commonly used as the antiviral therapeutic agents such as (S)-HPMPC [5], PMEA [6], (R)-PMPA [7], and d4AP [8]. Some acyclic nucleoside

* Corresponding author.

** Corresponding author.

E-mail addresses: fwliu@zzu.edu.cn (F.-W. Liu), wangcong@zzu.edu.cn (C. Wang).

phosphonates have been reported to have anticancer activity also such as PMEAs [9], (S)-HPMPC [10], and PMEDAP [11]. But only a few of anticancer cyclic nucleoside phosphonates have been reported such as BCH-1868 [12].

Threose nucleic acid (TNA) has received considerable interest as a possible RNA progenitor because of the chemical simplicity of threose relative to that of ribose and the ability of TNA to form thermally stable duplexes with DNA and RNA that are comparable to those of natural nucleic acid associations [13]. Moreover, Piet Herdewijn and co-workers [14] have demonstrated that the L-2'-deoxythreose nucleoside phosphonates PMDTA ($EC_{50} = 2.5 \mu\text{M}$) and PMDTT ($EC_{50} = 6.59 \mu\text{M}$) selectively inhibit HIV without affecting normal cell proliferation (Fig. 1). And also, they demonstrated that the diphosphate of PMDTA is an efficient selective substrate for HIV-1 reverse transcriptase. Being interested in the nucleoside phosphonate with modification of the L-threose skeleton, and as a part of continuous research on the SAR of L-threosyl nucleoside phosphonate, 4(R)-methyl-3-O-phosphonomethyl- α -L-threose nucleosides were designed and synthesized. Bioactivity of these target nucleoside phosphonates was evaluated as well. One amongst them was found to be a potent inhibitor against proliferation of breast cancer cells.

We herein describe the synthesis of a series of 4-methylthreose nucleoside phosphonates with various base moieties starting from D-xylose and the evaluation of their potential antitumour activities, particularly against the human breast cancer. We also disclose the mechanism of the potential compound **8g**, 1-(6-amino-2-fluoropurin-9-yl)-4-methyl-3-O-phosphonomethyl-L-threose, against MCF-7 and MDA-MB-231 tumour cell lines. In general, most of the modified nucleoside analogs are incorporated into the DNA or RNA molecules of tumor cells or viruses, which interfere with cell replication, competitively inhibit DNA polymerase and other functions, specifically interfere with nucleic acid synthesis and cause DNA damage [15]. DNA damage activates the cell cycle checkpoint, leading to cell cycle arrest and waiting for DNA repair. When DNA damage cannot be repaired, apoptosis is triggered, eventually leading to cell death. Therefore we investigated the effects of **8g** at different concentrations on antiproliferation, colony formation, cell cycle arrest, mitochondrial membrane potential and cell apoptosis in human breast cancers. Furthermore, in order to explore the anti-tumor mechanism of **8g**, we investigated the effects of **8g** on the expression of DNA damage proteins, cell cycle arrest proteins, PI3K/AKT signaling pathway proteins, and apoptosis pathway proteins. In summary, our study provides evidence for the use of **8g** as a promising anti-breast cancer compound.

2. Results and discussion

2.1. Chemistry

The target 4-methyl-3-O-phosphonomethyl-L-threose nucleosides **8a-8h** were synthesized via a multistep synthetic protocol starting from commercially available D-xylose. Firstly, selective protection of both hydroxyl groups at C-1 and C-2 of D-xylose with an isopropylidene group allowed 1,2-O-isopropylidene-D-xylose (**1**). The free primary hydroxyl group at C-5 was then tosylated to give **2** and following reductive elimination furnished intermediate **3**. The phosphonate function is introduced using the tosylate of diethylphosphonmethanol and NaH in THF to give 1,2-O-isopropylidene-4-methyl-3-O-phosphonomethyl-L-threose (**4**). Compound **5** was obtained by acid hydrolysis of **4** in aqueous acetic acid. Subsequent acetylation of 1,2-dihydroxyl groups of **5** with acetic anhydride in pyridine provided L-threose precursor **6** as illustrated in Scheme 1.

The precursor **6** was glycosidated via Vorbrüggen reaction with silylated uracil in presence of SnCl_4 , then the acetyl group was removed by saturated methanolic ammonia to yield **7a**. Further hydrolysis of the diethyl protecting groups with (TMS)Br at room temperature gave **8a**. However, when silylated thymine and silylated N^4 -benzoylcytosine were used in the Vorbrüggen glycosidation separately, corresponding protected nucleosides (**7b** and **7c**) were not obtained (Scheme 2).

Alternation of the glycosidation conditions were made to attempt synthesis of other target nucleosides using intermediate **6**. When compound **6** was treated with thymine, 5-chlorouracil, and 2-fluoroadenine in the presence of N,O-bis(trimethylsilyl)acetamide (BSA) and trimethylsilyl trifluoromethanesulfonate (TMSOTf) at room temperature, the reaction did not work. While the reaction mixture was heated to 65°C , newly generated spots with higher polarity were observed by monitored on TLC. After completion of the reaction, purification give corresponding products in low yields. Further structural elucidation showed that the product were 2-O-acetyl-3-O-ethylphosphonomethyl-L-threose nucleoside. One ethyl group was removed in the higher temperature. In consideration of the low yield of the reaction and the difficulty in purification, another alternative approach is needed in the further synthesis.

It is known that 2-O-benzoyl sugar precursor possesses more reactivity than 2-O-acetyl counterpart in the glycosylation because the benzoyl group could give a more stable five-membered cyclic transition state. Therefore 2-O-benzoyl-L-threose intermediate **11** was prepared using a three-step sequence from **4**. Firstly, treatment

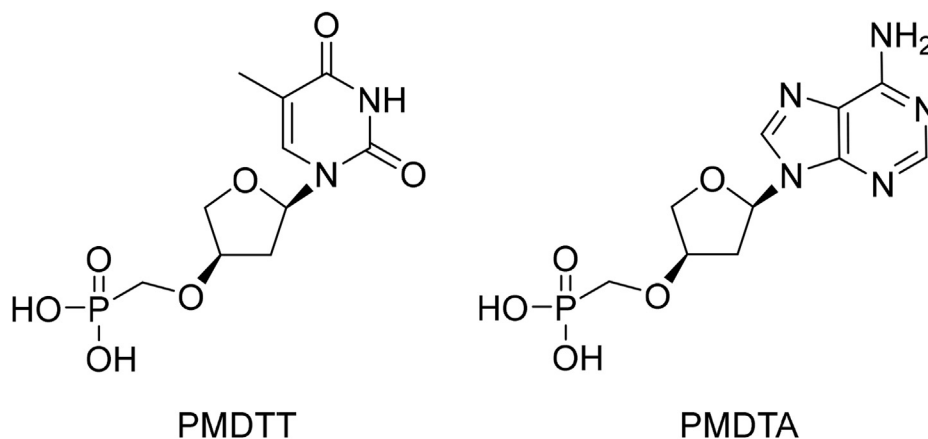
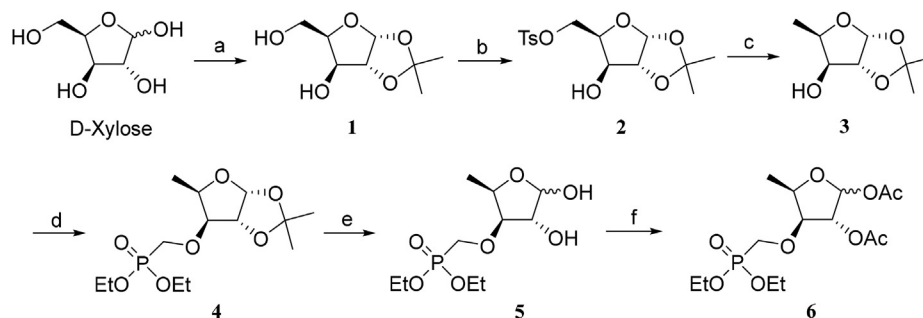
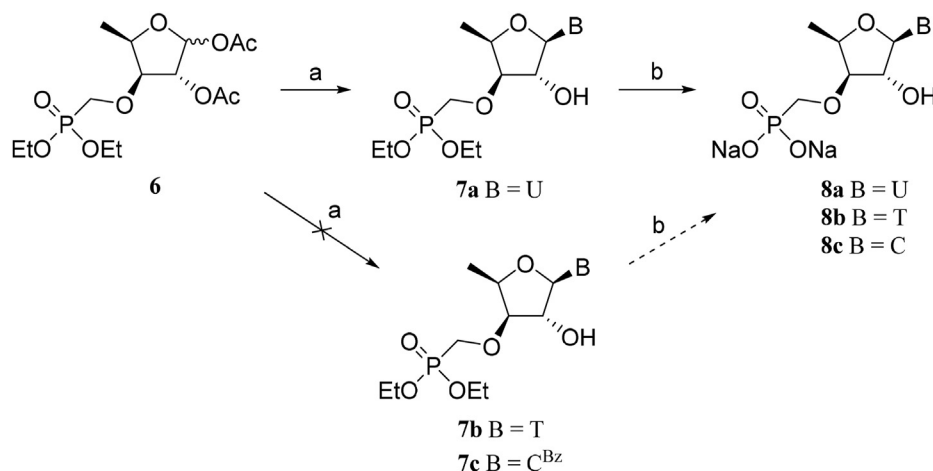


Fig. 1. Structure of PMDTT and PMDTA



Scheme 1. Synthesis of precursor **6**. (a) acetone, conc. H_2SO_4 ; aqueous NaOH ; (b) TsCl , pyridine, 67% from D -xylose (two steps); (c) LiAlH_4 , THF, 94%; (d) tosylate of diethylphosphonmethanol, NaH , THF, 83%; (e) 60% AcOH ; (f) Ac_2O , pyridine, 75% from **4** (two steps).



Scheme 2. Synthesis of **8a-8c**. (a) 1) silylated nucleobase, SnCl_4 , MeCN ; 2) saturated NH_3 in MeOH , 52%; (b) $(\text{TMS})\text{Br}$, 2,6-dimethylpyridine, MeCN , aqueous NaHCO_3 , 55%.

of 1,2-O-isopropylidene intermediate **4** with methanol under catalysis of sulfuric acid allowed methyl glycoside **9**. Then hydroxyl group at C-2 of **9** was benzoylated with benzoyl chloride to give **10**. Finally transformation of 1-methoxy group of **9** into 1-acetoxy group with acetic acid and acetic anhydride provided **11** (Scheme 3).

Glycosidation of precursor **11** with various nucleobases as starting materials in the presence of BSA/TMSOTf , and following a sequence of deprotections, allowed the desired nucleosides **8b-8h** successfully as described in Scheme 4.

2.2. Biology

2.2.1. Screening anticancer activity

The anticancer activity of the target nucleoside phosphonate analogs (**8a-8h**) was preliminarily screened in a human cervical carcinoma cell line (HeLa), a human breast cancer cell line (MCF-7), and a human gastric cancer cell line (MGC-803) by employing the MTT assay, respectively. The cells were treated with the test compounds for 72 h. The results are presented in Table 1.

Based on the preliminary results of the evaluations, we noticed that **8g** was the most active compound in all three cell lines among the eight compounds tested. Therefore further in vitro evaluation of compound **8g** was performed on eight cancer cell lines, including human lung adenocarcinoma cell line (A549), HeLa cell line, human colon cancer cell line (SW620), human esophageal carcinoma cell line (EC109), human prostate cancer cell line (PC3), human gastric epithelial cell lines (MGC-803) and human breast cancer cell lines (MDA-MB-231, MCF-7), and normal cell line GES-1. 5-Fluorouracil

(5-FU) was used as a positive control. The cells were treated with the test compounds for 72 h. The results are summarized in Table 2.

As shown in Table 2, compound **8g** exhibited potent inhibitory activity against all cancer cell lines with IC_{50} values in the 0.391–6.621 μM range, particularly the human breast cancer cell lines MCF-7 and MDA-MB-231 with IC_{50} values of 0.476 and 0.391 μM , respectively, representing 41- and 47-fold higher potency than the reference compound 5-FU. Furthermore, compound **8g** was less sensitive to GES-1, showing certain selectivity between normal and human breast cancer cells.

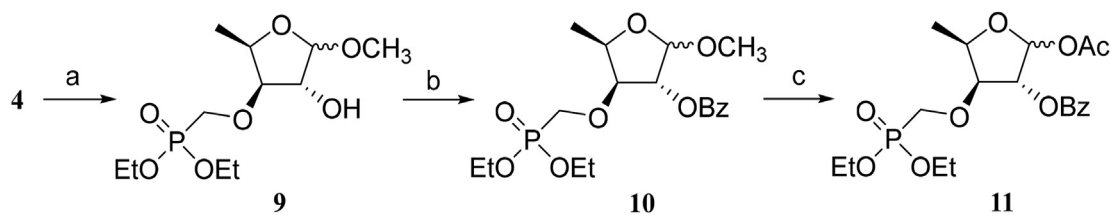
2.2.2. The inhibitory effects of compound 8g on breast cancer cells

MTT assays were used to test the antiproliferative effects of compound **8g** on breast cancer cells. As shown in Fig. 2(A), cell viability decreased with prolonging drug treatment time (24, 48 and 72 h) and increasing the concentration of compound **8g**.

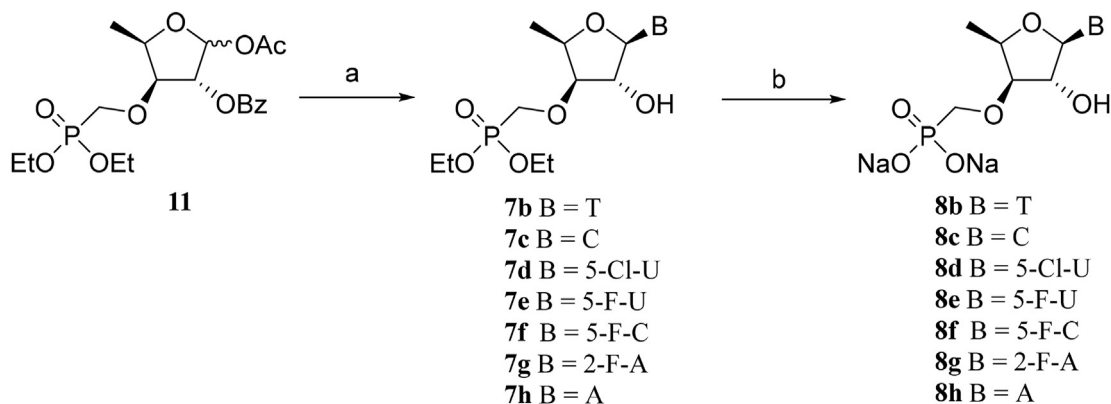
The inhibitory effect of **8g** on MCF-7 and MDA-MB-231 cells was detected by colony formation assay. As shown in Fig. 2(B), the number of cell clones decreased significantly with increasing **8g** concentration. The results revealed that the colony formation of breast cancer cells was inhibited in a concentration-dependent manner.

2.2.3. Cell cycle analysis by flow cytometry

The cell cycle profile of exponentially growing MCF-7 and MDA-MB-231 cells treated with compound **8g** for 48 h was analyzed by flow cytometry in cells stained with propidium iodide. Untreated cells served as a control. The results are presented in Fig. 3. After exposure of the cells to compound **8g** at different concentrations



Scheme 3. Synthesis of sugar precursor **11**. (a) MeOH, H₂SO₄; (b) benzoyl chloride, pyridine; (c) AcOH, Ac₂O, H₂SO₄, 55% from compound **4** (three steps).



Scheme 4. Synthesis of target compound **8b-8h** from precursor **11**. (a) 1) BSA, TMSOTf, MeCN, nucleobase; 2) saturated methanolic ammonia; (b) (TMS)Br, 2,6-dimethylpyridine, MeCN, aqueous NaHCO₃.

Table 1
Preliminary results of anticancer activity IC₅₀ (μM) of compounds **8a-8h**.

	8a	8b	8c	8d	8e	8f	8g	8h
HeLa	>16	>16	>16	>16	>16	>16	<8	>16
MCF-7	>16	>16	>16	>16	>16	>16	<8	>16
MGC-803	>16	>16	>16	>16	>16	>16	<8	>16

Table 2
The IC₅₀ of **8g** on the proliferation of cancer cell lines and normal cell line.

Cell lines	IC ₅₀ (μM)	
	Compound 8g	5-FU
A549	3.483 ± 0.297	—
Hela	6.195 ± 0.507	—
SW620	6.621 ± 0.565	—
EC109	2.566 ± 0.030	—
PC3	2.206 ± 0.192	—
MGC-803	6.178 ± 1.320	—
MDA-MB-231	0.391 ± 0.089	16.117 ± 2.550
MCF-7	0.476 ± 0.055	22.439 ± 0.951
GES-1	5.095 ± 0.328	—

for 48 h, the percentage of cells in G2/M phase relative to the control was increased as the concentration increased, showing that **8g** induced G2/M cell cycle arrest in both the MCF-7 and MDA-MB-231 cell lines.

2.2.4. Detection of apoptosis by flow cytometry

The effect of compound **8g** on the apoptosis of two human breast cancer cell lines was investigated using Annexin V-FITC/PI. After treatment with different concentrations of compound **8g** (0, 1, 2 and 4 μM for MCF-7 cells; 0, 3, 6 and 9 μM for MDA-MB-231 cells) for 48 h, cells were stained with PI and FITC and then analyzed by flow cytometry. As illustrated in Fig. 4, compound **8g** induced

apoptosis of both cell lines in a concentration-dependent manner. The total apoptosis percentage of MCF-7 cells changed from 3.6% to 76.1% with increasing concentrations of **8g** from 0 to 4 μM, and from 1.3% to 40.8% for MDA-MB-231 cells with increasing concentrations of **8g** from 0 to 9 μM.

2.2.5. Effects of compound **8g** on the mitochondrial membrane

JC-1 is an ideal fluorescent probe widely used to detect mitochondrial membrane potential. The decrease in mitochondrial membrane potential is a landmark detection indicator in the early stage of apoptosis [16]. MCF-7 and MDA-MB-231 breast cancer cells were treated with different concentrations of compound **8g**. After 48 h, the cells were collected, the samples were processed, and the reagents of the JC-1 detection kit were incubated at 37 °C for 20 min after staining. The instrument detects JC-1 in MCF-7 and MDA-MB-231 cells. As shown in Fig. 5, it can be seen from the flow histogram that as the concentration of compound **8g** increases, the mitochondrial membrane potential within the two cells gradually decreases.

2.2.6. Effects of compound **8g** on DNA damage/repair-related proteins and cell cycle-related proteins

ATM plays a vital role in maintaining the stability of the genome. When ATM is activated by DNA damage, it can phosphorylate the corresponding downstream proteins Chk1 and Chk2 to regulate cell cycle checkpoints, induce cell cycle arrest, and finally repair DNA damage [17]. But when DNA damage cannot be repaired, the apoptotic process is triggered. The results are shown in Fig. 6. As the concentration of compound **8g** increased, the protein expression of ATM, p-Chk2, Chk1, and Chk2 was upregulated. In addition, the expression of protein cdc25c was up-regulated and the protein CyclinB1 and p-cdc2 were down-regulated. These results indicate that compound **8g** can induce DNA damage to reach G2/M cycle arrest in breast cancer cells.

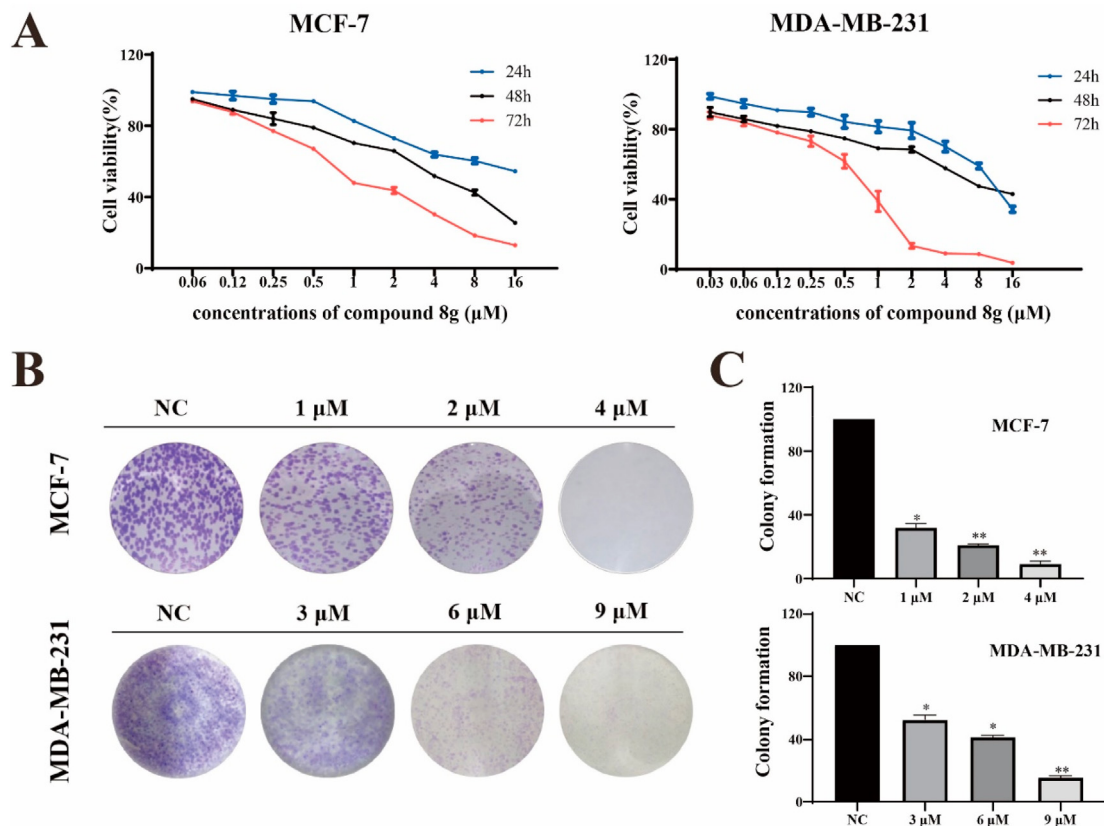


Fig. 2. (A) The inhibitory effect of compound **8g** in breast cancer cells. (B) Colony formation breast cancer cells after treatment with compound **8g** for 7 days. (C) The results shown are representative of three independent experiments. * $p < 0.05$, ** $p < 0.01$.

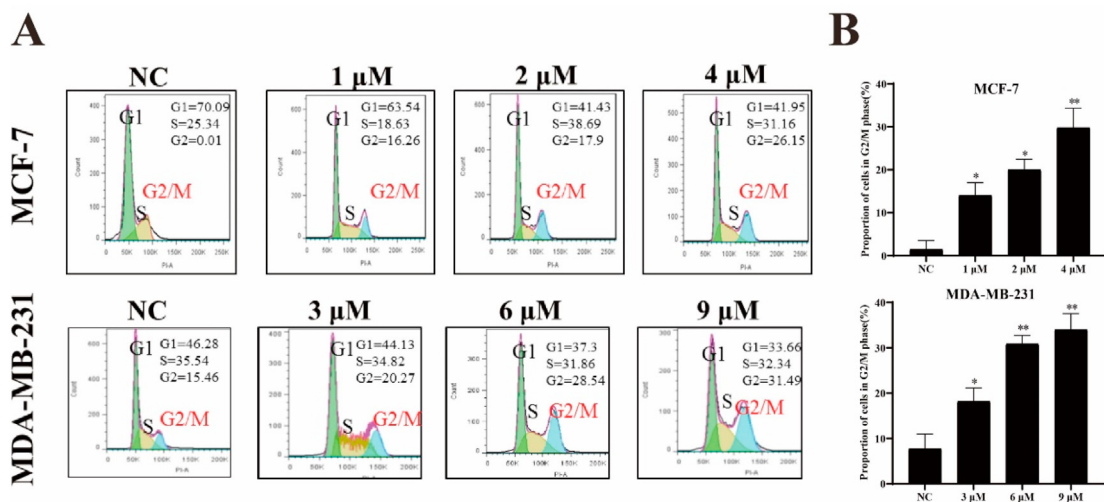


Fig. 3. (A) Flow cytometry detection of G2/M phase cells after 48 h of treatment of breast cancer cells with compound **8g**. (B) The results shown are representative of three independent experiments. * $p < 0.05$, ** $p < 0.01$.

2.2.7. Effects of compound 8g on apoptosis-related proteins

DNA damage activates the cell cycle checkpoint, leading to cell cycle arrest and waiting for DNA repair. When DNA damage cannot be repaired, apoptosis is triggered, eventually leading to cell death [18]. To explore the specific molecular mechanism of the effects of **8g** on apoptosis, we measured the expression levels of PARP, Cleaved PARP, Cleaved caspase3, Cleaved caspase7, Cleaved caspase9, Bax, Bcl-2, Bad, Noxa and Mcl-1 in MCF-7 and MDA-MB-

231 cells using Western blotting. As shown in Fig. 7, as the concentration of compound **8g** increased, the protein expression of the antiapoptotic protein Mcl-1 decreased, and the protein expression of the proapoptotic proteins Bad and Noxa increased, which caused the proportion of Bax/Bcl-2 protein to increase. This result shows that **8g** regulates Bcl-2 family protein expression, thereby reducing the mitochondrial membrane potential and ultimately inducing apoptosis of breast cancer cells. The expression levels of Cleaved

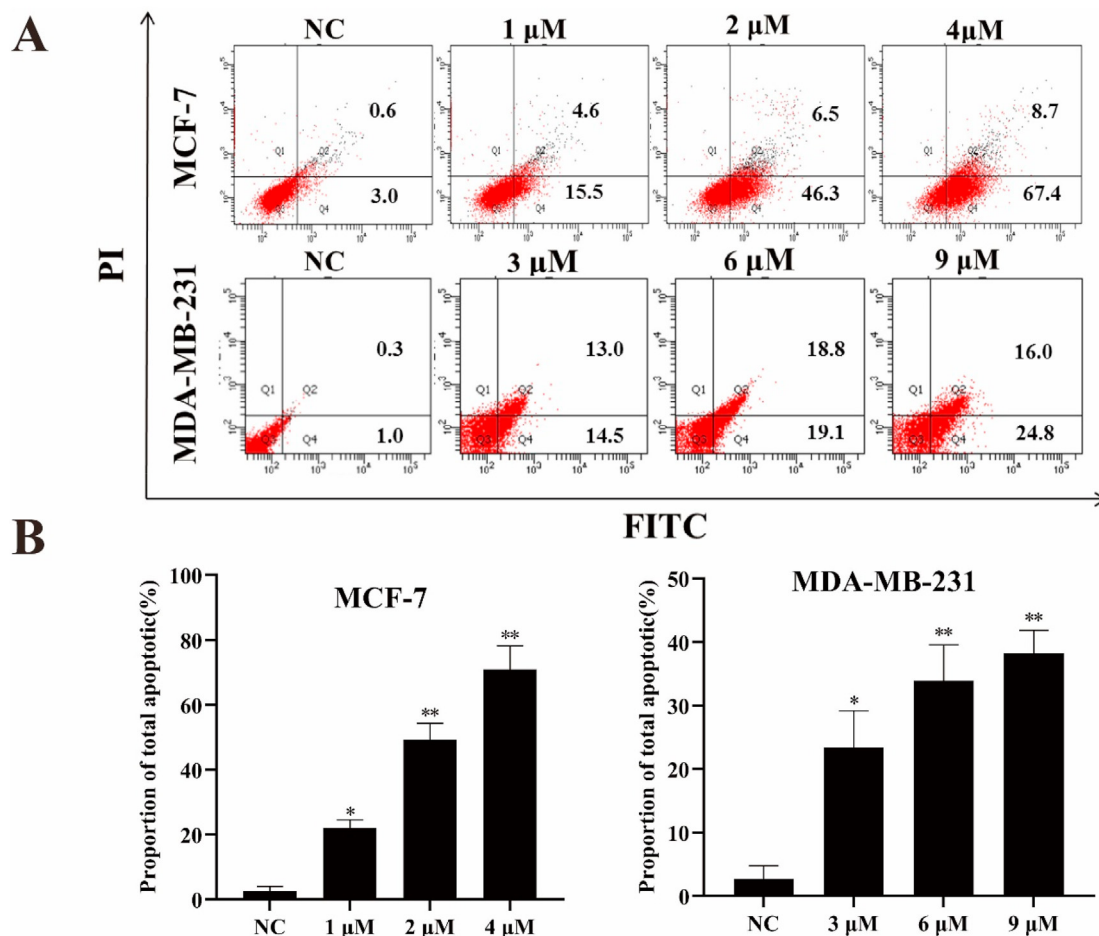


Fig. 4. The apoptosis rate of MCF-7 cells and MDA-MB-231 cells was determined by Annexin V-FITC/PI dual-staining assay. (A) MCF-7 cells were treated with compound **8g** (0, 1, 2 and 4 μM) for 48 h, MDA-MB-231 cells were treated with compound **8g** (0, 3, 6 and 9 μM) for 48 h, and flow cytometry analysis was performed after staining with Annexin V-FITC/PI. (B) The results shown are representative of three independent experiments. * $p < 0.05$, ** $p < 0.01$.

caspase9, Cleaved caspase3, Cleaved caspase7, and Cleaved PARP all increased with increasing drug concentration. These results indicate that compound **8g** can induce apoptosis of breast cancer cells.

2.2.8. Effects of compound **8g** on PI3K/Akt pathway-related proteins in breast cancer cells

The PI3K/Akt signalling pathway is a classic antiapoptotic pro-survival signalling pathway that is widely present in cells. After being activated in the PI3K/Akt pathway, activated Akt can phosphorylate downstream related anti-apoptotic factors, such as Caspase 3 of the Caspase family and Mcl-1 factor of the Bcl-2 family to promote survival. However, when the PI3K/Akt signalling pathway is inhibited, it will correspondingly inhibit downstream anti-apoptotic factors and activate downstream apoptotic factors to play a proapoptotic role [19]. MCF-7 and MDA-MB-231 breast cancer cells were treated with different concentrations of compound **8g**. After 48 h, the cells were collected, and proteins were extracted for Western blotting. The results are shown in Fig. 8. As the concentration of compound **8g** increased, protein ^{85a}p-Akt and ^{Ser473}p-PI3K expression was downregulated. These results indicate that compound **8g** can inhibit the expression of PI3K/Akt pathway-related proteins in breast cancer cells.

2.2.9. Effects of NSC663284 on compound **8g** on the cell cycle and apoptosis

NSC663284 can inhibit the phosphorylation of protein

phosphatase cdc25c at the Ser216 site, allowing p-cdc25c to accumulate in the nucleus, and finally activate the CyclinB-cdc2 complex to allow mitosis to proceed normally [20]. According to the above situation, we set up four groups of experiments (NC, **8g** group, 0.3 μM NSC663284 group, combination drug group) and detected the cell cycle by flow cytometry after 48 h in two breast cancer cell lines. It can be seen from Fig. 9(A), that when a high concentration of compound **8g** was added, the number of cells in the G2/M phase of the cell cycle was significantly increased. When the inhibitor NSC663284 was added, the number of cells in the G2/M phase of the cell cycle was significantly reduced (similar to the NC group). These results indicate that when the protein phosphatase cdc25c is inhibited, the G2/M phase cycle blockade caused by compound **8g** is converted to normal cell division. It was proven that compound **8g** induces G2/M phase cycle arrest of breast cancer cells through the ATM-Chk1/Chk2-cdc25c pathway.

According to the above situation, we set up four groups of experiments (NC, **8g** group, 0.3 μM NSC663284 group, combined drug group). The apoptosis of MCF-7 and MDA-MB-231 cells was detected by flow cytometry after 48 h. It can be seen from Fig. 9(B) that when the high concentration of compound **8g** was added, the number of apoptotic cells increased significantly. When the inhibitor NSC663284 was added, the number of apoptotic cells decreased significantly (similar to the NC group). It was proven that the inhibitor NSC663284 can inhibit the proapoptotic effect of compound **8g**.

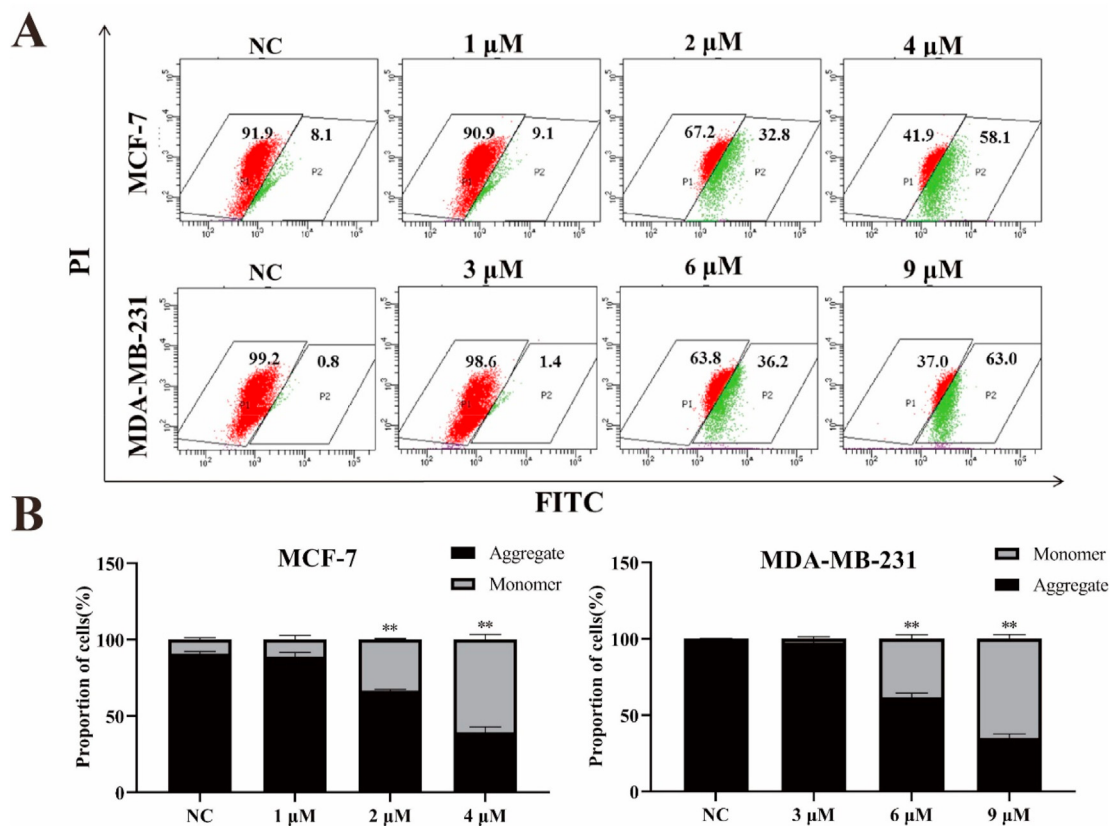


Fig. 5. Mitochondrial membrane potential dissipation induced by compound **8g**. (A) Flow cytometry analysis of the cellular mitochondrial membrane potential level of breast cancer cells treated with JC-1 and compound **8g** for 48 h. (B) The results shown are representative of three independent experiments. * $p < 0.05$, ** $p < 0.01$.

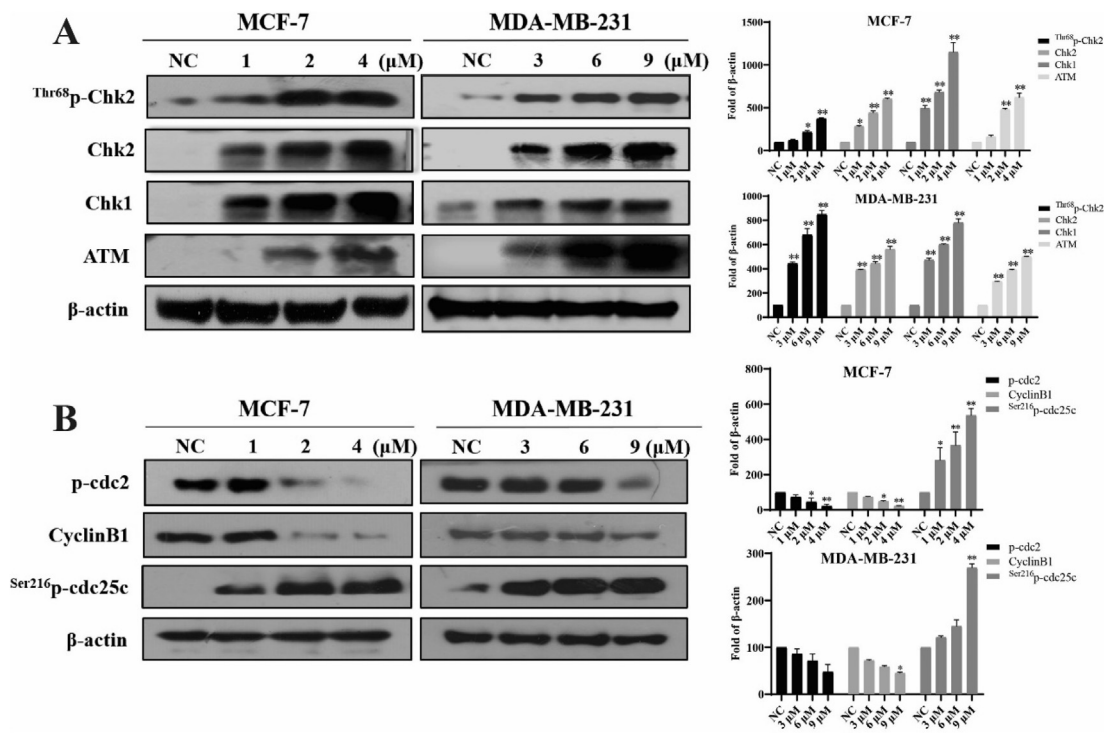


Fig. 6. Compound **8g** induced activation of the DNA damage response and G2/M phase arrest. (A) Total and phosphorylated proteins associated with the DNA damage response in MCF-7 and MDA-MB-231 cells treated with the indicated concentrations of compound **8g** for 48 h were analyzed by western blotting. (B) The expression of G2/M phase-related proteins was detected by western blotting. The results shown are representative of three independent experiments. * $p < 0.05$, ** $p < 0.01$.

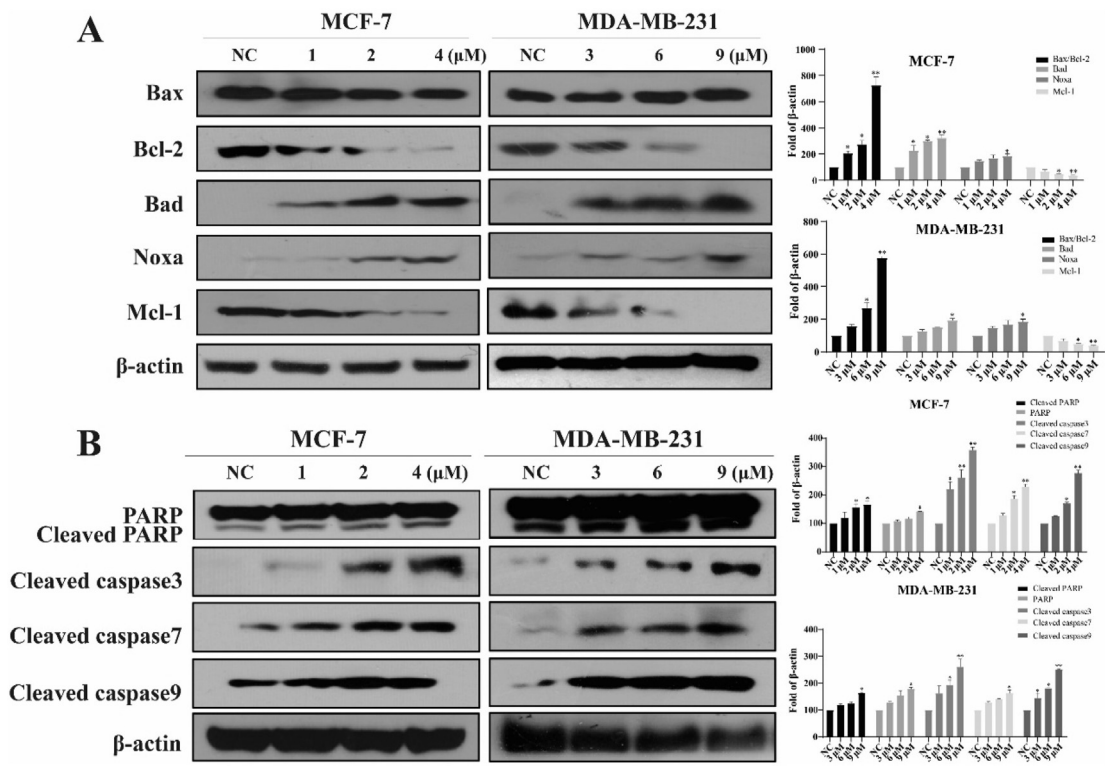


Fig. 7. (A) The protein levels of Bax, Bcl-2, Bad, Noxa, and Mcl-1 in MCF-7 and MDA-MB-231 cells incubated with various concentrations of **8g**. (B) The expression of Cleaved caspase3, Cleaved caspase7, Cleaved caspase9, PARP and Cleaved PARP in MCF-7 and MDA-MB-231 cells after treatment with various concentrations of **8g** for 48 h **p* < 0.05, ***p* < 0.01.

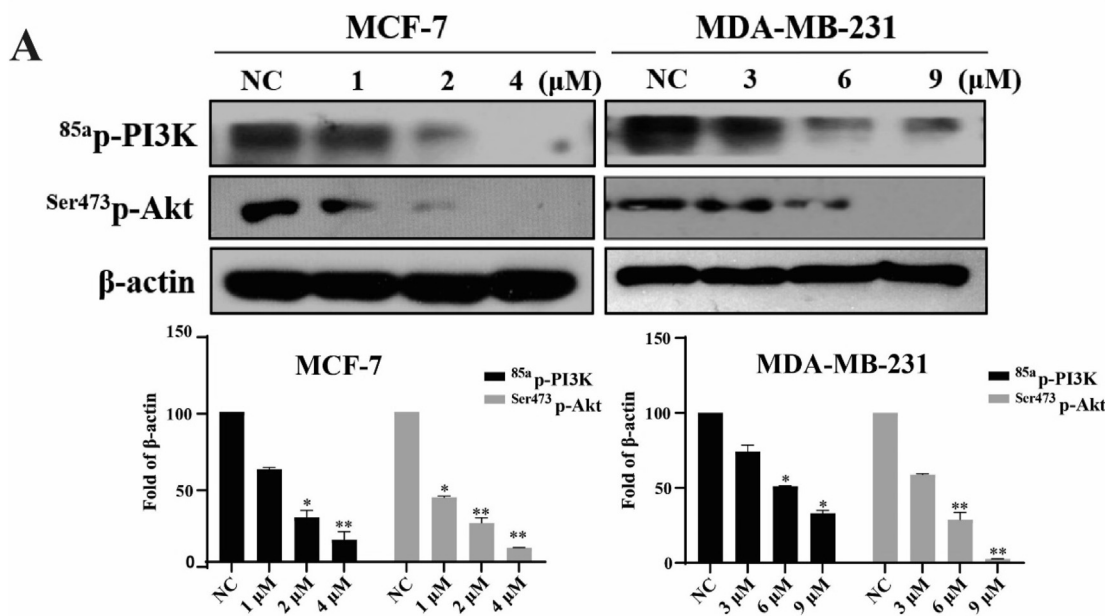


Fig. 8. (A) Effect of compound **8g** on the levels of PI3K/Akt pathway-related proteins in the breast cancer cell. (compared with the NC group, **P* < 0.05, ***P* < 0.01).

2.2.10. NSC663284 affects the protein expression changes of compound **8g in the cell cycle pathway and apoptotic pathway**

From the above results, we know that compound **8g** caused G2/M cycle arrest in breast cancer cells. According to the above situation, we set up four groups of experiments (NC, **8g** group, NSC663284 group with 0.3 μM added alone, combined drug group).

Fig. 10(A) shows that when a high concentration of compound **8g** was added, the expression of protein cdc25c was significantly upregulated, and the expression of protein cdc25c and protein p-cdc2 was significantly downregulated. However, when the inhibitor NSC663284 was added to the cells, the expression of protein cdc25c was significantly downregulated, and the expression of

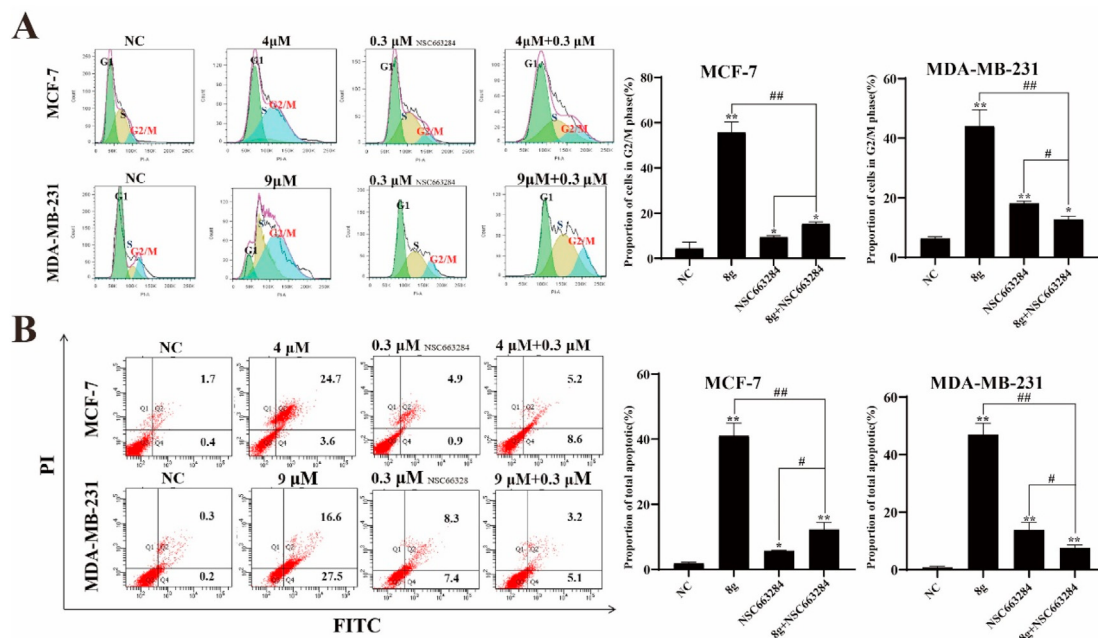


Fig. 9. (A) Detection of the cell cycle following treatment with compound **8g** and inhibitors for 48 h in breast cancer cells (compared to the NC group, $*P < 0.05$, $**P < 0.01$; compared with the combination treatment group, $\#P < 0.05$, $\#\#P < 0.01$). (B) Flow cytometry was used to detect the apoptosis of breast cancer cells after treatment with compound **8g** and inhibitors for 48 h (compared with the NC group, $*P < 0.05$, $**P < 0.01$; compared with the combination treatment group, $\#P < 0.05$, $\#\#P < 0.01$).

protein cdc25c and protein p-cdc2 was significantly upregulated (similar to the results of the NC group). This result shows that the high concentration of compound **8g** can promote the G2/M phase cycle arrest of breast cancer cells, but when the inhibitor NSC663284 is added, the cells gradually return to normal mitosis, indicating that the inhibitor NSC663284 can attenuate compound **8g**. Once again, it was proven that compound **8g** caused DNA damage to breast cancer cells through the ATM-Chk1/Chk2-cdc25c pathway, leading to blockage of the G2/M phase of breast cancer cells.

We know that compound **8g** can induce apoptosis of breast cancer cells. According to the above situation, we set up four groups of experiments (NC, **8g** group, 0.3 μ M NSC663284 group, combination drug group) and extracted proteins from two breast cancer cell lines after 48 h for Western blot experiments. Fig. 10(B) shows that when a high concentration of compound **8g** was added, the expression of caspase family-related proteins was significantly increased. When the inhibitor NSC663284 was added, the expression of caspase family-related proteins was significantly reduced (similar to the results of the NC group). The results show that a high concentration of compound **8g** can effectively promote the apoptosis of breast cancer cells, but when the inhibitor NSC663284 is added, the number of apoptotic cells is significantly reduced, indicating that the inhibitor NSC663284 can inhibit the proapoptotic effect of compound **8g**. It was proven again that compound **8g** caused DNA damage to breast cancer cells through the ATM-Chk1/Chk2-cdc25c pathway, leading to blockage of the G2/M phase cycle of breast cancer cells, which ultimately led to apoptosis.

3. Conclusion

Overall, novel 4-methyl- α -L-threose nucleoside phosphonate analogs were synthesized starting from D-xylose via a multistep sequence of reactions and evaluated for their activities against eight selected human cancer cell lines and a normal human cell line. Among all of the compounds, compound **8g** was found to possess the best antiproliferative activity in human breast cancer cells.

Further mechanistic studies indicated that compound **8g** mainly relied on causing DNA damage, inducing cell cycle arrest in G2/M phase, inhibiting the PI3K/Akt pathway, and ultimately inducing apoptosis. Compound **8g** regulates downstream apoptosis by downregulating p-cdc2 and CyclinB1, upregulating the G2/M phase key protein Ser^{216} p-cdc25c during cell cycle arrest, and downregulating 85a p-PI3K and Ser^{473} p-Akt in the PI3K/AKT pathway. Cdc25c plays an important role in regulating the G2/M phase of the cell cycle. Increased phosphorylation activity of cdc25c can activate the cdc2/CyclinB complex, promote the cell cycle and promote mitosis. NSC663284 can inhibit the phosphorylation of protein phosphatase cdc25c at the Ser216 site, allowing p-cdc25c to accumulate in the nucleus, and finally activate the CyclinB-cdc2 complex to allow mitosis to proceed normally. NSC663284 can reverse the promotion effect of **8g** on Ser^{216} p-cdc25c protein expression. Therefore, it is speculated that **8g** may target Ser^{216} p-cdc25c protein and block the cell cycle in the G2/M phase. In addition, **8g** can also inhibit cell proliferation by inhibiting the PI3K/AKT pathway. Moreover, **8g** further upregulated Bad and Noxa and downregulated Bcl-2 and Mcl-1, which ultimately led to the release of cytochrome C. Finally, caspase 9, caspase 7, caspase 3, and PARP were activated to induce cell apoptosis. In addition, NSC663284, an inhibitor of phosphorylation of the protein phosphatase cdc25c, reversed cell cycle arrest in G2/M phase and apoptosis caused by **8g**. These results indicate that compound **8g** holds promising potential as an antiproliferative agent with low toxicity.

4. Experimental

4.1. General

All reagents except anhydrous solvents were commercially available and used without further purification. Dichloromethane and acetonitrile was distilled over CaH_2 . THF was refluxed over sodium and distilled. All reactions were conducted under an inert atmosphere of nitrogen. ^1H and ^{13}C NMR spectra were recorded for samples in $\text{DMSO-}d_6$ or CDCl_3 or D_2O on a Bruker Avance III 400

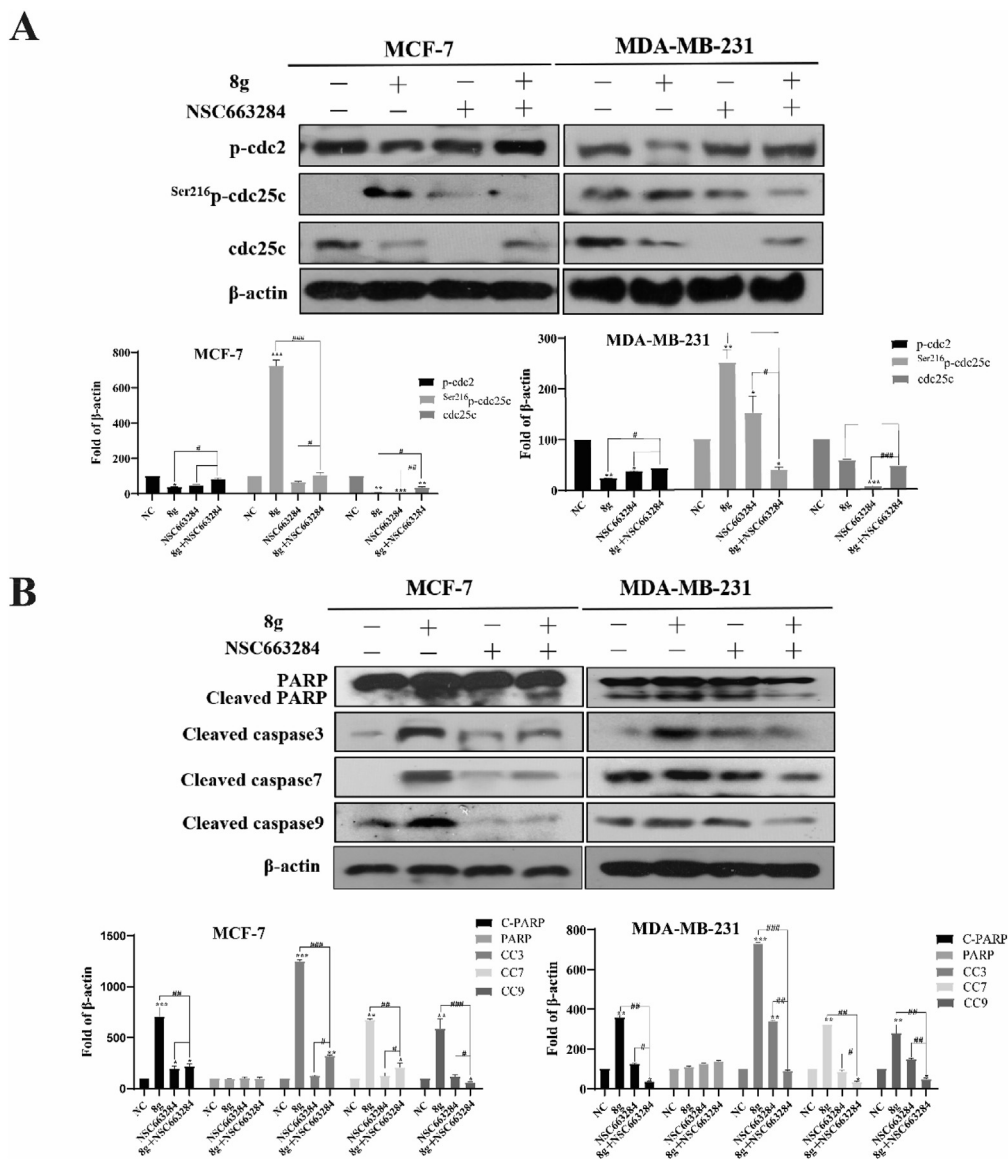


Fig. 10. (A) Effect of compound **8g** and inhibitor on cell cycle-related protein expression in breast cancer cells (compared with the NC group, * $P < 0.05$, ** $P < 0.01$; compared with the combination group, # $P < 0.05$, ## $P < 0.01$). (B) Effect of compound **8g** and inhibitors on the expression of caspase family-related proteins in breast cancer cells (compared to the NC group, * $P < 0.05$, ** $P < 0.01$; compared with the combination group, # $P < 0.05$, ## $P < 0.01$).

Digital NMR Spectrometer. High resolution mass spectra (HRMS) were recorded under electrospray ion conditions using a Q-ToF Micromass spectrometer. Thin-layer chromatography (TLC) was performed on silica gel GF254 with detection by charring with 5% phosphomolybdic acid in alcohol or by UV light. Melting points were determined on a XT5B melting-point apparatus and are uncorrected. Optical rotations were measured on a Perkin–Elmer 341 Polarimeter. Column chromatography was conducted on a column of silica gel (200–300 mesh). All phosphonates were purified by C-18 column chromatography eluting with H₂O/MeOH or H₂O/MeCN. Fraction solutions were lyophilized.

4.2. Chemical synthesis

4.2.1. 1,2-O-Diacetyl-4(R)-methyl-3-O-(diethylphosphonomethyl)-L-threose (**6**)

To a suspension of D-xylose (10 g, 66.7 mmol) in acetone (100 mL) was slowly added dropwise 98% sulfuric acid (8 mL) under

cooling in ice-water bath. Then the cooling bath was removed, the mixture was stirred at room temperature until disappearance of D-xylose by TLC detection. The pH value of the reaction mixture was adjusted to 1–2 by dropwise addition of 30% aqueous sodium hydroxide. After stirring at ambient temperature for 2 h, solid sodium hydroxide was added to the solution to adjust pH to 8.0. The resultant mixture was concentrated under reduced pressure to almost dryness. The residue was dispersed into acetone (80 mL) and filtrated. The filtrate was dried over Na₂SO₄ and concentrated in vacuo to give crude 1,2-O-isopropylidene-D-xylose **1** as a colorless oil.

The crude **1** was dissolved in anhydrous pyridine (100 mL) and *p*-toluenesulfonyl chloride (11 g, 58 mmol) was added in portions at 0 °C. The reaction mixture was warmed to 10 °C and stirred for 14 h. The reaction was quenched with saturated NaHCO₃ and concentrated in vacuo. The residue was partitioned between H₂O (50 mL) and EtOAc (100 mL). The organic layer was dried over Na₂SO₄ and concentrated in vacuo. The residue was purified by

chromatography on a silica gel column (EtOAc:PE = 1:2, R_f = 0.2) to afford 5-O-tosyl-1,2-O-isopropylidene- β -xylose **2** (15.3 g, 67% from β -xylose) as a white solid. mp 127.4–127.9 °C (literature [21]: 134–135 °C); ^1H NMR (400 MHz, CDCl_3) δ 7.81 (d, J = 8.3 Hz, 2H), 7.36 (d, J = 8.0 Hz, 2H), 5.88 (d, J = 3.6 Hz, 1H), 4.51 (d, J = 3.6 Hz, 1H), 4.40–4.26 (m, 3H), 4.14 (q, J = 9.0 Hz, 1H), 2.46 (s, 3H), 2.40 (d, J = 5.1 Hz, 1H), 1.46 (s, 3H), 1.30 (s, 3H). ^{13}C NMR (101 MHz, CDCl_3) δ 145.3, 132.4, 130.0, 128.0, 112.1, 105.0, 85.0, 76.7, 74.3, 66.2, 26.8, 26.2, 21.7 (Identical with NMR data in the literature [21]).

To a solution of **2** obtained above (10.0 g, 29.0 mmol) in dry THF (100 mL) was slowly added lithium aluminum hydride (1.65 g, 43.4 mmol) at 0 °C in three portions. The mixture was continued to stir vigorously under N_2 until disappearance of **2**. The reaction was quenched cautiously with water (5 mL) at 0 °C, and followed by dropwise addition of 15% aqueous sodium hydroxide (5 mL). After stirring for 30 min, the resultant slurry was filtered and the filtrate was concentrated in vacuo. The residue was purified by chromatography on a silica gel column (EtOAc:PE = 1:2, R_f = 0.25) to afford 5-deoxy-1,2-O-isopropylidene- β -xylose **3** (4.73 g, 94%) as a white solid. mp 72.8–73.1 °C (literature [21]: 81–83 °C); ^1H NMR (400 MHz, CDCl_3) δ 5.89 (d, J = 3.8 Hz, 1H), 4.53 (d, J = 3.8 Hz, 1H), 4.32 (qd, J = 6.5, 2.5 Hz, 1H), 3.99 (s, 1H), 1.50 (s, 3H), 1.31 (s, 3H), 1.30 (d, J = 6.5 Hz, 3H). ^{13}C NMR (101 MHz, CDCl_3) δ 111.4, 104.4, 85.5, 76.4, 75.9, 26.6, 26.1, 12.7 (Identical with the NMR data in the literature [21]).

To a solution of **3** (3.48 g, 20 mmol) in dried THF (50 mL) was added sodium hydride (80% dispersion in mineral oil, 1.2 g, 40 mmol) at 0 °C under N_2 . Then the solution of the tosylate of diethylphosphonmethanol (12.9 g, 40 mmol) in dried THF (50 mL) was dropwise added, and the reaction mixture was slowly warmed to room temperature. After being stirred for 6 h, the reaction was quenched with saturated NaHCO_3 and concentrated. The residue was partitioned between H_2O (40 mL) and DCM (80 mL). The organic layer was washed with water and brine, dried over Na_2SO_4 , and concentrated. The residue was purified by chromatography on a silica gel column (EtOAc:PE = 1:1, R_f = 0.20) to offer 5-deoxy-3-O-(diethylphosphonomethyl)-1,2-O-isopropylidene- β -xylose **4** (5.35 g, 83%) as a light yellow oil. ^1H NMR (400 MHz, CDCl_3) δ 5.76 (d, J = 4.0 Hz, 1H), 4.51 (d, J = 4.0 Hz, 1H), 4.33 (qd, J = 9.1, 4.6 Hz, 1H), 4.11–4.04 (m, 4H), 3.82 (dd, J = 13.6, 8.8 Hz, 1H), 3.72 (dd, J = 13.6, 7.6 Hz, 1H), 3.69 (d, J = 2.4 Hz, 1H), 1.38 (s, 3H), 1.23 (m, 12H). ^{13}C NMR (101 MHz, CDCl_3) δ 111.2, 104.6, 86.0 (d, $J_{\text{C-P}}$ = 9.2 Hz), 82.3, 75.9, 64.2 (d, $J_{\text{C-P}}$ = 168.1 Hz), 62.5 (d, $J_{\text{C-P}}$ = 14.6 Hz), 26.5, 26.1, 16.4 (d, $J_{\text{C-P}}$ = 5.2 Hz), 12.9.

The compound **4** (8.0 g, 24.7 mmol) was dissolved in 60% aqueous acetic acid (40 mL), the mixture was heated to 70 °C and stirred for 18 h at this temperature. The resultant solution was concentrated in vacuo. The residue was dissolved in EtOAc (60 mL), dried over anhydrous Na_2SO_4 , and concentrated to give **5** as a yellowish oil. To the oily **5** was added pyridine (30 mL) and acetic anhydride (10 mL). The mixture was stirred at ambient temperature under N_2 for 6 h. The reaction was quenched with saturated NaHCO_3 and concentrated in vacuo. The residue was partitioned between H_2O (50 mL) and EtOAc (100 mL). The organic layer was washed with brine twice, dried over anhydrous Na_2SO_4 , and concentrated in vacuo. The residue was purified by silica gel chromatography (EtOAc:PE = 1:1, R_f = 0.20) to offer 1,2-O-diacetyl-4(R)-methyl-3-O-(diethylphosphonomethyl)- β -threose **6** as a colorless oily mixture of α - and β -anomers (6.8 g, 75%). ^1H NMR (400 MHz, CDCl_3) δ 6.35 (d, J = 4.7 Hz, 1H), 6.05 (s, 1H), 5.20 (t, J = 4.3 Hz, 2H), 4.50–4.42 (m, 2H), 4.23–4.12 (m, 10H), 4.05 (dd, J = 9.2, 13.9 Hz, 1H), 3.95 (dd, J = 9.2, 13.9 Hz, 1H), 3.89 (dd, J = 8.0, 13.9 Hz, 1H), 3.83 (dd, J = 8.3, 13.8 Hz, 1H), 2.11 (s, 3H), 2.10 (s, 3H), 2.09 (s, 3H), 2.07 (s, 3H), 1.36 (d, J = 6.5 Hz, 3H), 1.35 (t, J = 7.0 Hz, 12H), 1.30 (t, J = 6.5 Hz, 3H). ^{31}P NMR (162 MHz, CDCl_3) δ 21.12,

21.05.

4.2.2. 1-(Uracil-1-yl)-4(R)-methyl-3-O-(diethylphosphonomethyl)- β -threose (7a)

Uracil (0.403 g, 3.6 mmol) was dissolved in anhydrous toluene (25 mL), ammonia sulfate (10 mg, 0.07 mmol) and HMDS (20 mL) were added at room temperature under nitrogen. The mixture was refluxed overnight and then concentrated in vacuo. To the residue was added the solution of **6** (0.663 g, 1.8 mmol) in 15 mL of dry MeCN followed by a dropwise addition of SnCl_4 (840 μL , 7.2 mmol). The reaction mixture was stirred for 4 h at ambient temperature. The reaction was quenched with saturated aqueous NaHCO_3 and concentrated to dryness. The residue was dispersed in 30 mL of DCM and filtered. The cake was washed with DCM (20 mL) twice. The combined organic layer was dried over Na_2SO_4 , and concentrated to yield a syrup. To the syrup was added saturated methanolic ammonia (15 mL), the mixture was stirred at room temperature overnight and evaporated. The residue was purified by chromatography on a silica gel column (DCM:MeOH = 30:1) to afford **7a** (0.351 g, 0.93 mmol, 52%) as a yellowish oil. R_f = 0.40 (DCM:MeOH = 10:1). ^1H NMR (400 MHz, CDCl_3) δ 7.54 (d, J = 8.2 Hz, 1H), 5.69 (s, 1H), 5.64 (d, J = 8.2 Hz, 1H), 4.54–4.38 (m, 1H), 4.31 (s, 1H), 4.05 (dq, J = 14.0, 7.1 Hz, 4H), 3.88–3.62 (m, 3H), 1.43–1.31 (m, 3H), 1.34–1.20 (m, 6H). ^{13}C NMR (101 MHz, CDCl_3) δ 164.3, 151.0, 140.8, 101.4, 91.8, 86.2 (d, $J_{\text{C-P}}$ = 10.5 Hz), 78.9, 78.4, 63.4 (d, $J_{\text{C-P}}$ = 167 Hz), 62.5 (d, $J_{\text{C-P}}$ = 6.9 Hz), 62.4 (d, $J_{\text{C-P}}$ = 6.9 Hz), 16.2 (d, $J_{\text{C-P}}$ = 5.4 Hz), 13.1. ^{31}P NMR (162 MHz, CDCl_3) δ 20.7. HRMS: calcd. for $\text{C}_{14}\text{H}_{24}\text{N}_2\text{O}_8\text{P}$ $[\text{M}+\text{H}]^+$: 379.1265, found: 379.1268.

4.2.3. 1-O-Acetyl-2-O-benzoyl-3-O-diethylphosphonomethyl-4(R)-methyl- β -threose (11)

To the solution of **4** (10 g, 31 mmol) in methanol (100 mL) was dropwise added concentrated sulfuric acid (1.6 mL, 30 mmol) under cooling in an ice-water bath, the mixture was stirred for 14 h, then solid NaHCO_3 was added slowly. When carbon dioxide was not continued to be generated, addition was stopped. The mixture was concentrated to dryness, and EtOAc (50 mL) was added. The organic layer was dried over Na_2SO_4 and concentrated to offer **9** as a colorless oil.

The compound **9** obtained above was dissolved in absolute pyridine (80 mL), and benzoyl chloride (7 mL, 60 mmol) was dropwise added under cooling in an ice-water bath. The mixture was warmed to room temperature and stirred for 4 h, then the reaction was quenched with saturated aqueous NaHCO_3 and concentrated. The residue was partitioned between EtOAc and saturated brine. The organic layer was dried over Na_2SO_4 and concentrated. The residue was purified by chromatography on a silica gel column (PE:EtOAc = 1:1, R_f = 0.20) to allow methyl 2-O-benzoyl-4-methyl-3-O-diethylphosphonomethyl- β -threopentofuranoside **10** as a colorless oily mixture of two anomers. ^1H NMR (400 MHz, CDCl_3) δ 8.13–8.00 (m, 4H), 7.63–7.55 (m, 2H), 7.00–7.42 (m, 4H), 5.32 (s, 1H), 5.21 (d, J = 4.5 Hz, 1H), 5.13 (t, J = 4.5 Hz, 1H), 5.02 (s, 1H), 4.53–4.41 (m, 2H), 4.35 (dd, J = 6.3, 4.6 Hz, 1H), 4.23–4.09 (m, 9H), 4.07 (d, J = 5.0 Hz, 1H), 4.01–3.93 (m, 2H), 3.85 (dd, J = 13.7, 8.8 Hz, 1H), 3.43 (s, 3H), 3.34 (s, 3H), 1.39 (d, J = 6.6 Hz, 3H), 1.36–1.27 (m, 15H). ^{13}C NMR (101 MHz, CDCl_3) δ 165.9, 165.5, 133.5, 133.4, 129.8, 129.7, 129.4, 129.3, 128.51, 128.47, 107.2, 100.2, 84.6 (d, $J_{\text{C-P}}$ = 8.9 Hz), 84.2 (d, $J_{\text{C-P}}$ = 11.7 Hz), 80.9, 79.3, 78.0, 73.2, 64.3 (d, $J_{\text{C-P}}$ = 167.4 Hz), 64.1 (d, $J_{\text{C-P}}$ = 165.7 Hz), 62.64 (d, $J_{\text{C-P}}$ = 5.3 Hz), 62.61 (d, $J_{\text{C-P}}$ = 5.3 Hz), 62.5 (d, $J_{\text{C-P}}$ = 5.3 Hz), 62.4 (d, $J_{\text{C-P}}$ = 5.3 Hz), 55.5, 55.4, 16.55–16.36 (m), 15.5, 14.9. ^{31}P NMR (162 MHz, CDCl_3) δ 20.4, 20.0.

The compound **10** obtained above was dissolved in acetic acid (100 mL), acetic anhydride (9.5 mL, 100 mmol) and H_2SO_4 (65 μL , 1.25 mmol) was added in sequence at 0 °C. The mixture was stirred

at room temperature for 8 h, quenched with saturated aqueous NaHCO₃ and then partitioned between EtOAc and water. The organic layer was dried over Na₂SO₄ and concentrated. The residue was purified by chromatography on a silica gel column (PE:EtOAc = 1:1, R_f = 0.20) to afford **11** (7.33 g, 55% from **4**) as a colorless oily mixture of two anomers (anomer-1: anomer-2 = 1:0.6). Anomer-1: ¹H NMR (400 MHz, CDCl₃) δ 8.05–8.00 (m, 2H), 7.63–7.58 (m, 1H), 7.60–7.43 (m, 2H), 6.23 (s, 1H), 5.45 (t, J = 4.4 Hz, 1H), 4.60–4.51 (m, 1H), 4.24–4.10 (m, 5H), 4.07 (d, J = 5.0 Hz, 1H), 3.97 (dd, J = 13.7, 7.9 Hz, 1H), 2.12 (s, 3H), 1.41 (d, J = 6.6 Hz, 3H), 1.35 (t, J = 7.1 Hz, 6H). Anomer-2: ¹H NMR (400 MHz, CDCl₃) δ 8.05–8.00 (m, 2H), 7.63–7.58 (m, 1H), 7.60–7.43 (m, 2H), 6.49 (d, J = 4.6 Hz, 1H), 5.45 (t, J = 4.4 Hz, 1H), 4.60–4.51 (m, 1H), 4.24–4.10 (m, 5H), 4.03 (dd, J = 13.9, 8.9 Hz, 1H), 3.90 (dd, J = 13.9, 8.1 Hz, 1H), 1.99 (s, 3H), 1.35 (d, J = 6.6 Hz, 3H), 1.31 (t, J = 7.1 Hz, 6H). ¹³C NMR (101 MHz, CDCl₃) δ 169.8, 165.35, 165.35, 165.31, 133.8, 133.6, 129.8, 129.7, 129.1, 128.9, 128.6, 99.5, 94.0, 84.04 (d, J_{C-P} = 10.0 Hz), 84.03 (d, J_{C-P} = 10.1 Hz), 80.3, 79.6, 77.2, 76.1, 64.3 (d, J_{C-P} = 167.2 Hz), 62.7–62.5 (m), 21.2, 20.9, 16.6–16.4 (m), 15.0, 14.5. ³¹P NMR (162 MHz, CDCl₃) δ 20.1, 19.9.

4.2.4. 1-(Thymin-1-yl)-4(R)-methyl-3-O-(diethylphosphonomethyl)-α-L-threose (**7b**)

Thymine (48 mg, 0.38 mmol), N,O-bis(trimethylsilyl)acetamide (196 μL, 0.8 mmol), compound **11** (108 mg, 0.25 mmol), and 10 mL of MeCN were added to a dried flask. The mixture was heated in an oil bath maintained at 65 °C, until a clear solution was obtained. After the mixture was cooled down to room temperature, trimethylsilyl trifluoromethanesulfonate (200 μL, 1.1 mmol) was added with stirring under N₂. As soon as completion of addition, the temperature was raised to 65 °C again and maintained for 4 h. The reaction was quenched with saturated aqueous NaHCO₃ and concentrated in vacuo. MeOH (30 mL) was added to the residue, and stirred for 10 min. Resultant mixture was filtered and washed with 10 mL of MeOH. The combined filtrate was dried over Na₂SO₄ and concentrated in vacuo to give a syrup. The syrup was dissolved in 15 mL of saturated methanolic ammonia, stirred at room temperature overnight and evaporated. The residue was separated by chromatography on a silica gel column (DCM:MeOH = 20:1, R_f = 0.15) to afford **7b** as a yellowish oil. ¹H NMR (400 MHz, DMSO-*d*₆) δ 11.33 (s, H), 7.36 (d, J = 1.2 Hz, 1H), 5.85 (d, J = 4.4 Hz, 1H), 5.71 (d, J = 1.6 Hz, 1H), 4.28–4.23 (m, 1H), 4.16 (s, 1H), 4.10–3.98 (m, 5H), 3.88 (dd, J = 13.6, 8.8 Hz, 1H), 3.70 (d, J = 3.2 Hz, 1H), 1.80 (d, J = 0.8 Hz, 3H), 1.29 (d, J = 6.4 Hz, 3H), 1.25 (t, J = 6.8 Hz, 3H), 1.24 (t, J = 7.2 Hz, 3H). ¹³C NMR (101 MHz, DMSO-*d*₆) δ 163.7, 150.5, 136.5, 109.3, 90.1, 86.5 (d, J_{C-P} = 12.7 Hz), 77.8, 77.2, 63.1 (d, J_{C-P} = 164.7 Hz), 61.8 (d, J_{C-P} = 6.3 Hz), 61.7 (d, J_{C-P} = 6.3 Hz), 16.3 (d, J_{C-P} = 5.4 Hz), 13.3, 12.2. ³¹P NMR (162 MHz, DMSO-*d*₆) δ 20.8. HRMS: calcd. for C₁₄H₂₅N₃O₇P [M+H]⁺: 393.1421, found: 393.1426.

4.2.5. 1-(Cytosin-1-yl)-4(R)-methyl-3-O-(diethylphosphonomethyl)-α-L-threose (**7c**)

Compound **11** (108 mg, 0.25 mmol) was treated with N⁴-benzoylcytosine (80 mg, 0.37 mmol) according to the procedure as described in 4.2.4, to give compound **7c** (60 mg, 63%) as a foamy solid. R_f = 0.20 (DCM:MeOH = 10:1). ¹H NMR (400 MHz, DMSO-*d*₆) δ 7.51 (d, J = 7.6 Hz, 1H), 7.23 (s, 1H), 7.10 (s, 1H), 5.79 (d, J = 3.6 Hz, 1H), 5.73–5.73 (m, 2H), 4.32–4.26 (m, 1H), 4.09 (s, 1H), 4.05–3.97 (m, 4H), 3.91 (dd, J = 14.0, 9.2 Hz, 1H), 3.83 (dd, J = 14.0, 8.4 Hz, 1H), 3.68 (d, J = 3.2 Hz, 1H), 1.30 (d, J = 6.4 Hz, 3H), 1.24 (t, J = 6.8 Hz, 3H), 1.23 (t, J = 6.8 Hz, 3H). ¹³C NMR (101 MHz, DMSO-*d*₆) δ 165.5, 155.1, 141.4, 93.6, 91.3, 86.5 (d, J_{C-P} = 11.7 Hz), 77.9, 77.5, 63.0 (d, J_{C-P} = 164.1 Hz), 61.8 (d, J_{C-P} = 6.0 Hz), 16.3 (d, J_{C-P} = 5.5 Hz), 13.4. ³¹P NMR (162 MHz, CDCl₃) δ 20.7. HRMS: calcd. for C₁₄H₂₅N₃O₇P [M+H]⁺: 378.1425, found: 378.1426.

4.2.6. 1-(5-Chlorouracil-1-yl)-4(R)-methyl-3-O-(diethylphosphonomethyl)-α-L-threose (**7d**)

Compound **11** (108 mg, 0.25 mmol) was treated with 5-chlorouracil (56 mg, 0.38 mmol) according to the procedure as described in 4.2.4, to give compound **7d** (63 mg, 0.16 mmol, 63%) as a foamy solid. R_f = 0.4 (DCM:MeOH = 10:1). ¹H NMR (400 MHz, CDCl₃) δ 10.79 (s, 1H), 7.76 (s, 1H), 5.73 (s, 1H), 5.38 (d, J = 3.2 Hz, 1H), 4.56 (qd, J = 6.4, 3.2 Hz, 1H), 4.49 (d, J = 2.0 Hz, 1H), 4.19–4.10 (m, 4H), 3.90 (d, J = 8.8 Hz, 2H), 3.84 (d, J = 3.2 Hz, 1H), 1.47 (d, J = 6.8 Hz, 3H), 1.34 (t, J = 6.8 Hz, 3H), 1.33 (t, J = 7.2 Hz, 3H). ¹³C NMR (101 MHz, CDCl₃) δ 159.8, 150.2, 137.5, 108.4, 92.8, 86.0 (d, J_{C-P} = 10.0 Hz), 79.8, 78.5, 64.1 (d, J_{C-P} = 168.6 Hz), 62.9 (d, J_{C-P} = 6.5 Hz), 62.6 (d, J_{C-P} = 6.7 Hz), 16.5 (d, J_{C-P} = 3.0 Hz), 16.5 (d, J_{C-P} = 3.0 Hz), 13.3. ³¹P NMR (162 MHz, CDCl₃) δ 20.3. HRMS: calcd. for C₁₄H₂₃ClN₂O₈P [M+H]⁺: 413.0875, found: 413.0878.

4.2.7. 1-(5-Fluorouracil-1-yl)-4(R)-methyl-3-O-(diethylphosphonomethyl)-α-L-threose (**7e**)

Compound **11** (108 mg, 0.25 mmol) was treated with 5-fluorouracil (50 mg, 0.38 mmol) according to the procedure as described in 4.2.4, to give compound **7e** (59 mg, 0.15 mmol, 61%) as a foamy solid. R_f = 0.4 (DCM:MeOH = 10:1). ¹H NMR (400 MHz, CDCl₃) δ 10.74 (s, 1H), 7.65 (d, J = 6.4 Hz, 1H), 5.74 (s, 1H), 5.29 (s, 1H), 4.52 (qd, J = 6.4, 2.8 Hz, 1H), 4.45 (s, 1H), 4.20–4.06 (m, 4H), 3.90 (dd, J = 13.9, 9.4 Hz, 1H), 3.86 (dd, J = 13.9, 8.8 Hz, 1H), 3.81 (d, J = 3.2 Hz, 1H), 1.45 (d, J = 6.4 Hz, 3H), 1.33 (t, J = 7.0 Hz, 3H), 1.32 (t, J = 7.0 Hz, 3H). ¹³C NMR (101 MHz, CDCl₃) δ 157.6 (d, J_{C-F} = 26.5 Hz), 149.5, 140.3 (d, J_{C-F} = 235.7 Hz), 125.0 (d, J_{C-F} = 35.1 Hz), 92.5, 86.0 (d, J_{C-P} = 10.1 Hz), 79.6, 78.6, 64.0 (d, J_{C-P} = 168.7 Hz), 62.8 (d, J_{C-P} = 6.7 Hz), 62.6 (d, J_{C-P} = 6.7 Hz), 16.4 (d, J_{C-P} = 5.8 Hz), 13.3. ¹⁹F NMR (376 MHz, CDCl₃) δ 166.0. ³¹P NMR (162 MHz, CDCl₃) δ 20.3. HRMS: calcd. for C₁₄H₂₃FN₂O₈P [M+H]⁺: 397.1171, found: 397.1175.

4.2.8. 1-(5-Fluorocytosin-1-yl)-4(R)-methyl-3-O-(diethylphosphonomethyl)-α-L-threose (**7f**)

Compound **11** (129 mg, 0.3 mmol) was treated with 5-fluorocytosine (58 mg, 0.45 mmol) according to the procedure as described in 4.2.4, to give compound **7f** (64 mg, 56%) as a white solid. R_f = 0.3 (DCM:MeOH = 10:1). mp: 188.6–189.1 °C. ¹H NMR (400 MHz, DMSO-*d*₆) δ 7.72 (s, 1H), 7.52 (d, J = 6.8 Hz, 2H), 5.84 (d, J = 4.4 Hz, 1H), 5.65 (s, 1H), 4.30 (qd, J = 6.4, 3.2 Hz, 1H), 4.12 (d, J = 4.0 Hz, 1H), 4.06–3.95 (m, 4H), 3.92 (dd, J = 14.0, 9.6 Hz, 1H), 3.84 (dd, J = 13.6, 8.8 Hz, 1H), 3.66 (d, J = 2.8 Hz, 1H), 1.32 (d, J = 6.4 Hz, 3H), 1.24 (t, J = 7.0 Hz, 3H), 1.21 (t, J = 7.0 Hz, 3H). ¹³C NMR (101 MHz, DMSO-*d*₆) δ 157.9 (d, J_{C-F} = 13.5 Hz), 153.8, 136.3 (d, J_{C-F} = 241.6 Hz), 126.0 (d, J_{C-F} = 32.4 Hz), 92.1, 86.9 (d, J_{C-P} = 12.3 Hz), 78.3 (d, J_{C-P} = 16.0 Hz), 63.7 (d, J_{C-P} = 164.1 Hz), 63.3, 62.2 (d, J_{C-P} = 6.2 Hz), 16.7 (d, J_{C-P} = 5.7 Hz), 13.8. ¹⁹F NMR (376 MHz, DMSO-*d*₆) δ –167.8. ³¹P NMR (162 MHz, DMSO-*d*₆) δ 20.7. HRMS: calcd. for C₁₄H₂₄FN₃O₇P [M+H]⁺: 396.1330, found: 396.1333.

4.2.9. 1-(2-Fluoroadenin-1-yl)-4(R)-methyl-3-O-(diethylphosphonomethyl)-α-L-threose (**7g**)

Compound **11** (112 mg, 0.26 mmol) was treated with 2-fluoroadenine (60 mg, 0.39 mmol) according to the procedure as described in 4.2.4, to give compound **7g** (61 mg, 0.15 mmol, 58%) as a white solid. R_f = 0.25 (DCM:MeOH = 10:1). mp: 205.5–206.5 °C. ¹H NMR (400 MHz, DMSO-*d*₆) δ 8.09 (s, 1H), 7.84 (s, 2H), 6.04 (d, J = 4.4 Hz, 1H), 5.75 (s, 1H), 4.56 (s, 1H), 4.39 (m, 1H), 4.09–4.00 (m, 5H), 3.91 (dd, J = 14.0, 8.8 Hz, 1H), 3.85 (d, J = 3.2 Hz, 1H), 1.31 (d, J = 6.4 Hz, 3H), 1.25 (t, J = 6.8 Hz, 3H), 1.23 (t, J = 6.8 Hz, 3H). ¹³C NMR (101 MHz, DMSO-*d*₆) δ 158.7 (d, J_{C-F} = 205.0 Hz), 157.5 (d, J_{C-F} = 21.4 Hz), 150.4 (d, J_{C-F} = 20.2 Hz), 139.2 (d, J_{C-F} = 2.5 Hz), 116.9 (d, J_{C-F} = 3.9 Hz), 88.8, 86.4 (d, J_{C-P} = 12.0 Hz), 79.0, 77.8 (d, J_{C-P} = 13.7 Hz), 63.3 (d, J_{C-P} = 164.8 Hz), 61.8 (d, J_{C-P} = 6.4 Hz), 16.2 (d,

$J_{C-P} = 5.5$ Hz), 13.7. ^{19}F NMR (376 MHz, $\text{DMSO-}d_6$) $\delta -52.1$. ^{31}P NMR (162 MHz, $\text{DMSO-}d_6$) $\delta 20.6$. HRMS: calcd. for $\text{C}_{15}\text{H}_{24}\text{FN}_5\text{O}_6\text{P}$ $[\text{M}+\text{H}]^+$: 420.1443, found: 420.1445.

4.2.10. 1-(Adenin-1-yl)-4(R)-methyl-3-O-(diethylphosphonomethyl)- α -L-threose (7 h)

Compound **11** (112 mg, 0.26 mmol) was treated with adenine (53 mg, 0.39 mmol) according to the procedure as described in 4.2.4, to give compound **7h** (56 mg, 55%) as a white solid. $R_f = 0.25$ (DCM:MeOH = 10:1). mp: 183.5–184.0 °C. ^1H NMR (400 MHz, $\text{DMSO-}d_6$) δ 8.16 (s, 1H), 8.13 (s, 1H), 7.29 (s, 2H), 6.03 (d, $J = 4.00$ Hz, 1H), 5.89 (s, 1H), 4.58 (s, 1H), 4.40–4.38 (m, 1H), 4.12–3.98 (m, 5H), 3.92 (dd, $J = 13.7$, 8.9 Hz, 1H), 3.85 (d, $J = 2.4$ Hz, 1H), 1.31 (d, $J = 6.0$ Hz, 3H), 1.25 (t, $J = 6.9$ Hz, 3H), 1.23 (t, $J = 6.9$ Hz, 3H). ^{13}C NMR (101 MHz, $\text{DMSO-}d_6$) δ 155.9, 152.7, 149.2, 139.0, 118.4, 88.5, 86.4 (d, $J_{C-P} = 12.6$ Hz), 77.8, 77.5, 63.3 (d, $J_{C-P} = 164.3$ Hz), 61.8 (d, $J_{C-P} = 6.2$ Hz), 16.3 (d, $J_{C-P} = 5.4$ Hz), 13.8. ^{31}P NMR (162 MHz, $\text{DMSO-}d_6$) δ 20.8. HRMS: calcd. for $\text{C}_{15}\text{H}_{25}\text{N}_5\text{O}_6\text{P}$ $[\text{M}+\text{H}]^+$: 402.1537, found: 402.1540.

4.2.11. 1-(Uracil-1-yl)-4(R)-methyl-3-O-(phosphonomethyl)- α -L-threose disodium salt (8a)

To a solution of **7a** (100 mg, 0.26 mmol) in MeCN (5 mL) was added 2,6-dimethylpyridine (290 μL , 2.5 mmol) and bromotrimethylsilane (690 μL , 5.2 mmol) in sequence at 0 °C under N_2 . Then the reaction mixture was warmed to room temperature and stirred overnight. The reaction was quenched with saturated aqueous NaHCO_3 and concentrated. The residue was purified by a C-18 column (MeOH:H $_2$ O = 1:4) to offer **8a** (52 mg, 55%) as a white solid. $[\alpha]_D^{20} +5.83$ (c 0.34, H $_2$ O). ^1H NMR (400 MHz, D_2O) δ 7.77 (d, $J = 7.8$ Hz, 1H), 5.81 (d, $J = 7.8$ Hz, 1H), 5.85 (s, 1H), 4.40 (m, 1H), 4.38 (s, 1H), 3.87 (s, 1H), 3.46 (m, 2H), 1.36 (d, $J = 6.4$ Hz, 3H). ^{13}C NMR (101 MHz, D_2O) δ 171.3, 155.4, 142.4, 102.7, 90.1, 85.4 (d, $J_{C-P} = 8.2$ Hz), 78.8, 77.9, 67.8 (d, $J_{C-P} = 150$ Hz), 13.3. ^{31}P NMR (162 MHz, D_2O) δ 13.1. HRMS: calcd. for $\text{C}_{10}\text{H}_{14}\text{N}_2\text{O}_8\text{P}[\text{M}-2\text{Na} + \text{H}]^-$: 321.0493, found: 321.0493.

4.2.12. 1-(Thymin-1-yl)-4(R)-methyl-3-O-(phosphonomethyl)- α -L-threose disodium salt (8b)

Compound **7b** was hydrolyzed according to the procedure as described in 4.2.11 to afford **8b** as a white solid (33 mg, 35% from compound **11**). $[\alpha]_D^{20} -15.5$ (c 0.32, H $_2$ O). ^1H NMR (400 MHz, D_2O) δ 7.51 (d, $J = 1.1$ Hz, 1H), 5.77 (d, $J = 1.8$ Hz, 1H), 4.39 (dq, $J = 6.4$, 3.8 Hz, 1H), 4.33 (s, 1H), 3.77 (d, $J = 3.5$ Hz, 1H), 3.64 (dd, $J = 13.1$, 9.3 Hz, 1H), 3.54 (dd, $J = 13.1$, 9.5 Hz, 1H), 1.81 (t, $J = 0.76$ Hz, 3H), 1.36 (d, $J = 6.4$ Hz, 3H). ^{13}C NMR (101 MHz, D_2O) δ 166.5, 151.7, 138.0, 111.2, 90.4, 85.7 (d, $J_{C-P} = 11.8$ Hz), 79.2, 77.9, 65.9 (d, $J_{C-P} = 157.4$ Hz), 12.8, 11.6. ^{31}P NMR (162 MHz, D_2O) δ 15.1. HRMS: calcd. for $\text{C}_{11}\text{H}_{16}\text{N}_2\text{O}_8\text{P}[\text{M}-2\text{Na} + \text{H}]^-$: 335.0650, found: 335.0652.

4.2.13. 1-(Cytosin-1-yl)-4(R)-methyl-3-O-(phosphonomethyl)- α -L-threose disodium salt (8c)

Compound **7c** was hydrolyzed according to the procedure as described in 4.2.11 to afford **8c** as a white solid in 57% yield. $[\alpha]_D^{20} +12.0$ (c 0.33, H $_2$ O). ^1H NMR (400 MHz, D_2O) δ 7.73 (d, $J = 7.6$ Hz, 1H), 5.92 (d, $J = 7.6$ Hz, 1H), 5.78 (d, $J = 1.5$ Hz, 1H), 4.38 (dq, $J = 6.4$, 3.6 Hz, 1H), 4.29 (s, 1H), 3.75 (d, $J = 3.3$ Hz, 1H), 3.48 (dd, $J = 12.7$, 8.8 Hz, 2H), 3.40 (dd, $J = 12.7$, 9.2 Hz, 2H), 1.32 (d, $J = 6.4$ Hz, 3H). ^{13}C NMR (101 MHz, D_2O) δ 166.1, 157.6, 142.7, 96.1, 91.1, 85.4 (d, $J_{C-P} = 10.4$ Hz), 79.4, 77.8, 66.7 (d, $J_{C-P} = 154.4$ Hz), 12.9. ^{31}P NMR (162 MHz, D_2O) δ 13.3. HRMS: calcd. for $\text{C}_{10}\text{H}_{15}\text{N}_3\text{O}_7\text{P}[\text{M}-2\text{Na} + \text{H}]^-$: 320.0653, found: 320.0655.

4.2.14. 1-(5-Chlorouracil-1-yl)-4(R)-methyl-3-O-(phosphonomethyl)- α -L-threose disodium salt (8d)

Compound **7d** was hydrolyzed according to the procedure as described in 4.2.11 to afford **8d** as a white solid in 62% yield. $[\alpha]_D^{20} -25.5$ (c 0.27, H $_2$ O). ^1H NMR (400 MHz, D_2O) δ 7.80 (s, 1H), 5.77 (d, $J = 2.8$ Hz, 1H), 4.39–4.36 (m, 1H), 4.32 (s, 1H), 3.97 (s, 1H), 3.47–3.44 (m, 2H), 1.33 (d, $J = 6.4$ Hz, 3H). ^{13}C NMR (101 MHz, D_2O) δ 163.1, 151.7, 138.8, 108.8, 90.7, 85.1 (d, $J_{C-P} = 9.1$ Hz), 79.6, 77.9, 66.9 (d, $J_{C-P} = 153.7$ Hz), 13.1. ^{31}P NMR (162 MHz, D_2O) δ 14.6. HRMS: calcd. for $\text{C}_{10}\text{H}_{13}\text{ClN}_2\text{O}_8\text{P}[\text{M}-2\text{Na} + \text{H}]^-$: 355.0104, found: 355.0106.

4.2.15. 1-(5-Fluorouracil-1-yl)-4(R)-methyl-3-O-(phosphonomethyl)- α -L-threose disodium salt (8e)

Compound **7e** was hydrolyzed according to the procedure as described in 4.2.11 to afford **8e** as a white solid in 60% yield. $[\alpha]_D^{20} -10.4$ (c 0.29, H $_2$ O). ^1H NMR (400 MHz, D_2O) δ 7.85 (d, $J = 6.1$ Hz, 1H), 5.80 (s, 1H), 4.43–4.40 (m, 1H), 4.37 (s, 1H), 3.88 (s, 1H), 3.57–3.44 (m, 2H), 1.38 (d, $J = 6.3$ Hz, 3H). ^{13}C NMR (101 MHz, D_2O) δ 163.3 (d, $J_{C-F} = 21.2$ Hz), 153.3, 141.2 (d, $J_{C-F} = 237$ Hz), 125.8 (d, $J_{C-F} = 34.9$ Hz), 90.5, 85.2 (d, $J_{C-P} = 9.3$ Hz), 79.1, 78.0, 67.4 (d, $J_{C-P} = 151$ Hz), 13.1. ^{19}F NMR (376 MHz, D_2O) $\delta -164.6$. ^{31}P NMR (162 MHz, D_2O) δ 13.6. HRMS: calcd. for $\text{C}_{10}\text{H}_{13}\text{FN}_2\text{O}_8\text{P}[\text{M}-2\text{Na} + \text{H}]^-$: 339.0399, found: 339.0400.

4.2.16. 1-(5-Fluorocytosin-1-yl)-4(R)-methyl-3-O-(phosphonomethyl)- α -L-threose disodium salt (8f)

Compound **7f** was hydrolyzed according to the procedure as described in 4.2.11 to afford **8f** as a white solid in 59% yield. $[\alpha]_D^{20} +3.13$ (c 0.32, H $_2$ O). ^1H NMR (400 MHz, D_2O) δ 7.84 (d, $J = 6.3$ Hz, 1H), 5.74 (s, 1H), 4.41–4.39 (m, 1H), 4.31 (s, 1H), 3.82 (s, 1H), 3.48–3.35 (m, 2H), 1.36 (d, $J = 6.4$ Hz, 3H). ^{13}C NMR (101 MHz, D_2O) δ 158.4 (d, $J_{C-F} = 14.9$ Hz), 155.8, 137.4 (d, $J_{C-F} = 242.3$ Hz), 126.7 (d, $J_{C-F} = 32.7$ Hz), 91.3, 85.1 (d, $J_{C-P} = 8.9$ Hz), 79.6, 78.0, 67.3 (d, $J_{C-P} = 151.8$ Hz), 13.0. ^{19}F NMR (376 MHz, D_2O) $\delta -165.2$. ^{31}P NMR (162 MHz, D_2O) δ 13.4. HRMS: calcd. for $\text{C}_{10}\text{H}_{14}\text{N}_3\text{FO}_7\text{P}[\text{M}-2\text{Na} + \text{H}]^-$: 338.0559, found: 338.0562.

4.2.17. 1-(2-Fluoroadenin-1-yl)-4(R)-methyl-3-O-(phosphonomethyl)- α -L-threose disodium salt (8g)

Compound **7g** was hydrolyzed according to the procedure as described in 4.2.11 to afford **8g** as a white solid in 53% yield. $[\alpha]_D^{20} -56.9$ (c 0.28, H $_2$ O). ^1H NMR (400 MHz, D_2O) δ 8.12 (s, 1H), 5.72 (d, $J = 1.36$ Hz, 1H), 4.55 (s, 1H), 4.46 (m, 1H), 3.85 (dd, $J = 3.6$, 0.8 Hz, 1H), 3.63 (dd, $J = 13.1$, 9.3 Hz, 1H), 3.56 (dd, $J = 13.1$, 9.3 Hz, 1H), 1.33 (d, $J = 6.5$ Hz, 3H). ^{13}C NMR (101 MHz, D_2O) δ 158.7 (d, $J_{C-F} = 211.6$ Hz), 156.6 (d, $J_{C-F} = 16.5$ Hz), 149.6 (d, $J_{C-F} = 18.9$ Hz), 140.7, 116.1, 88.7, 85.7 (d, $J_{C-P} = 11.6$ Hz), 79.6, 78.1, 66.4 (d, $J_{C-P} = 157.4$ Hz), 13.1. ^{19}F NMR (376 MHz, D_2O) $\delta -53.1$. ^{31}P NMR (162 MHz, D_2O) δ 12.9. HRMS: calcd. for $\text{C}_{11}\text{H}_{14}\text{FN}_5\text{O}_6\text{P}[\text{M}-2\text{Na} + \text{H}]^-$: 362.0671, found: 362.0673.

4.2.18. 1-(Adenin-1-yl)-4(R)-methyl-3-O-(phosphonomethyl)- α -L-threose disodium salt (8 h)

Compound **7h** was hydrolyzed according to the procedure as described in 4.2.11 to afford **8h** as a white solid in 50% yield. $[\alpha]_D^{20} -9.04$ (c 0.33, H $_2$ O). ^1H NMR (400 MHz, D_2O) δ 8.35 (s, 1H), 8.05 (s, 1H), 5.88 (s, 1H), 4.68 (s, 1H), 4.50–4.47 (m, 1H), 3.97 (s, 1H), 3.50 (d, $J = 8.4$ Hz, 2H), 1.34 (d, $J = 6.8$ Hz, 3H). ^{13}C NMR (101 MHz, D_2O) δ 155.4, 152.6, 148.7, 141.0, 118.2, 87.8, 85.6 (d, $J_{C-P} = 9.4$ Hz), 79.2, 78.3, 68.4 (d, $J_{C-P} = 151.1$ Hz), 13.6. ^{31}P NMR (162 MHz, D_2O) δ 13.0. HRMS: calcd. for $\text{C}_{11}\text{H}_{15}\text{N}_5\text{O}_6\text{P}[\text{M}-2\text{Na} + \text{H}]^-$: 344.0765, found: 344.0768.

4.3. Cell culture

Human breast cancer cells (MCF-7) and (MDA-MB-231), esophageal cancer (EC109), lung cancer (A549), breast cancer (MCF-7), prostate cancer (PC3), cervical cancer (HeLa), colon cancer (SW620), stomach cancer (MGC-803) cell lines, human gastric epithelial cell line (GES-1), the above cells were purchased from China Center for Type Collection (CCTCC, China) and grown in RPMI-1640 medium (Corning, USA) with 10% fetal bovine serum (FBS). Cells were cultured in a humid atmosphere of 5% CO₂ and 95% air at 37 °C.

4.4. Determination of *in vitro* anticancer activity

For evaluating the cytotoxic effect of tested compounds. The cells were plated at a density of 3000 exponentially growing cells per well seeded into 96-well plate and incubated at 37 °C. After 12 h incubation, remove medium and add 200 μL fresh medium containing different concentration of candidate compounds to each well for another 72 h incubation. Then, 20 μL MTT solution (5 mg/mL) was added to each well and allowed to react for 4 h. Removal of the medium containing MTT, followed by addition of 150 μL DMSO to each well and agitation until the dark blue crystal was dissolved completely. Absorbance (A) was determined at 570 nm with a reference wavelength of 630 nm. Finally, calculate the relative percentage inhibition rate of viable cells.

4.5. Colony formation assay

Cancer cells were cultured at a density of 1×10^3 in six-well plates. After an overnight incubation, the medium was removed and the cells were treated with 3 mL fresh medium containing various concentrations of compound **8g** dissolved in DMSO for 24 h incubation. After 24 h, the medium was removed, the plates were incubated for another 7 days. After treatment, the cell colonies were washed twice by PBS, fixed with 4% paraformaldehyde for 30 min, and stained with 0.1% crystal violet for 30 min. After washing away the crystal violet with PBS, the plates were photographed and counted. Finally, the number of cell clones was analyzed using ImageJ.

4.6. Flow cytometry measure for cells apoptosis and cell cycle

For apoptotic assay, using different concentrations of compound **8g**, after 48 h treatment, cells were collected and used the AnnexinV-FITC/PI apoptosis kit (KeyGEN BioTECH, USA) according to the manufacturer's instructions to detect apoptosis cells. About ten thousand events were collected for each sample and were analyzed by flow cytometry (BD Bioscience, USA).

For cell cycle distribution assay, using different concentrations of compound **8g**, after 48 h treatment, the cells were collected and washed with ice-cold PBS, fixed with 70% ice-cold ethanol at 4 °C overnight. Before analyzed by Instrument LSRFortessa (BD Bioscience, USA), the cells were washed by PBS and stained with RNase and PI (KeyGEN BioTECH, USA) for 30 min in dark condition according to the protocol.

4.7. Detection of cell mitochondrial membrane potential

JC-1 Assay Kit was used to detect the changes of MMP. Breast cancer cells were inoculated in 6-well plate for 24 h and then treated with compound **8g** at the stated concentrations. After incubation, according to the manufacturer's instructions, the green fluorescence percentage from JC-1 monomers was detected by flow cytometry.

4.8. Western blot analysis

The effect of compound **8g** on the cell cycle and apoptosis of breast cancer was detected by Western blot. For example, the expression levels of DNA damage-related protein, cell cycle regulators, and apoptosis related proteins. The protein samples were separated by sodium dodecyl sulfate-polyacrylamide gel electrophoresis (SDS-PAGE; 5%–15% gels), with protein standards used as molecular weight markers. After electrophoresis, proteins were transferred to nitrocellulose filter membranes. The membranes were blocked with 5% nonfat-dried milk in phosphate-buffered saline with 0.1% Tween 20 for 2 h and incubated with primary antibodies overnight at 4 °C. After the primary antibodies had been incubated overnight, the membranes were washed three times in phosphate-buffered saline with 0.1% Tween 20 for 15 min, incubated with biotin-conjugated secondary antibodies for 1 h with gentle shaking, and washed again in phosphate-buffered saline with 0.1% Tween 20. Blots were visualized with X-ray film. Protein expression was measured with ImageJ software.

4.9. Statistical analysis

SPSS 18.0 statistical software was used for variance testing. All results were presented as mean ± standard deviation. The significance of difference between the control group and the three experimental groups was analyzed with one-way analysis of variance. Differences were considered to be statistically significant when $P < 0.05$. All of the analyses were performed with Graph Pad 8.0.

Declaration of competing interest

The authors declare that they have no known competing financial interests or personal relationships that could have appeared to influence the work reported in this paper.

Acknowledgements

This work was supported by Natural Science Foundation of Henan Province, China (No. 162300410281) and National Natural Science Foundation of China (No. U1904156).

Appendix A. Supplementary data

Supplementary data to this article can be found online at <https://doi.org/10.1016/j.ejmech.2021.113513>.

References

- [1] a) A. Holy, *Antivir. Res.* 71 (2006) 248–253;
b) E. De Clercq, In search of a selective antiviral chemotherapy, *Clin. Microbiol. Rev.* 10 (1997) 674–693.
- [2] A.R. Van Rompay, M. Johansson, A. Karlsson, *Pharmacol. Ther.* 87 (2000) 189–198.
- [3] U. Pradere, E.C. Garnier-Amblard, S.J. Coats, F. Amblard, R.F. Schinazi, *Chem. Rev.* 114 (2014) 9154–9218.
- [4] a) Y.-H. Koh, J.H. Shim, J.Z. Wu, W. Zhong, Z. Hong, J.-L. Girardet, *J. Med. Chem.* 48 (2005) 2867;
b) C. Liu, S.G. Dumbre, C. Pannecouque, C. Huang, R.G. Ptak, M.G. Murray, S. De Jonghe, P. Herdewijn, *J. Med. Chem.* 59 (2016) 9513–9531.
- [5] a) E. De Clercq, A. Holy, I. Rosenberg, T. Sakuma, J. Balzarini, P.C. Maudgal, *Nature* 323 (1986) 464–467;
b) M. Baba, S. Mori, S. Shigeta, E. De Clercq, *Antimicrob. Agents Chemother.* 31 (1987) 337–339.
- [6] R. Pauwels, J. Balzarini, D. Schols, M. Baba, J. Desmyter, I. Rosenberg, A. Holy, E. De Clercq, *Antimicrob. Agents Chemother.* 32 (1988) 1025–1030.
- [7] J. Balzarini, A. Holy, J. Jindrich, L. Naesens, R. Snoeck, D. Schols, E. De Clercq, *Antimicrob. Agents Chemother.* 37 (1993) 332–338.
- [8] a) C.U. Kim, B.Y. Luh, J.C. Martin, *J. Org. Chem.* 56 (1991) 2642–2647;
b) R.L. Mackman, C.G. Boojamra, V. Prasad, L. Zhang, K.Y. Lin, O. Petrakovsky,

- D. Babusis, J. Chen, J. Douglas, D. Grant, H.C. Hui, C.U. Kim, D.Y. Markevitch, J. Vela, A. Ray, T. Cihlar, *Bioorg. Med. Chem. Lett* 17 (2007) 6785–6789.
- [9] S. Hatse, L. Naesens, B. Degreve, C. Segers, M. Vandeputte, M. Waer, E. De Clercq, J. Balzarini, *Int. J. Canc.* 76 (1998) 595–600.
- [10] N. Wakisaka, T. Yoshizaki, N. Raab-Traub, J.S. Pagano, *Int. J. Canc.* 116 (2005) 640–645.
- [11] S. Hatse, L. Naesens, E. De Clercq, J. Balzarini, *Biochem. Pharmacol.* 58 (1999) 311–323.
- [12] L. Leblond, G. Attardo, B. Hamelin, D.Y. Bouffard, N. Nguyen-Ba, H. Gourdeau, *Mol. Canc. Therapeut.* 1 (2002) 737–746.
- [13] a) H.Y. Yu, S. Zhang, J.C. Chaput, *Nat. Chem.* 4 (2012) 183–187;
b) C. Liu, C. Cozens, F. Jaziri, J. Rozenski, A. Marechal, S. Dumbre, V. Pezo, P. Marliere, V.B. Pinheiro, E. Groaz, P. Herdewijn, *J. Am. Chem. Soc.* 140 (2018) 6690–6699.
- [14] T. Wu, M. Froeyen, V. Kempeneers, C. Pannecouque, J. Wang, R. Busson, E. De Clercq, P. Herdewijn, *J. Am. Chem. Soc.* 127 (2005) 5056–5065.
- [15] E. Scholar, in: S.J. Enna, D.B. Bylund (Eds.), *Antimetabolites. xPharm: the Comprehensive Pharmacology Reference*, Elsevier, New York, 2007, pp. 1–4.
- [16] M. Panda, S. Tripathi, B. Biswal, *Mol. Biol. Rep.* 47 (2020) 4155–4168.
- [17] H.L. Smith, H. Southgate, D.A. Tweddle, N.J. Curtin, *Expet Rev. Mol. Med.* 22 (2020) e2.
- [18] Z. Li, A.H. Pearlman, P. Hsieh, *DNA Repair* 38 (2016) 94–101.
- [19] a) J. Yang, C. Pi, G. Wang, *Biomed. Pharmacother.* 103 (2018) 699–707;
b) Z. Cao, Q. Liao, M. Su, K. Huang, J. Jin, D. Cao, *Canc. Lett.* 459 (2019) 30–40.
- [20] Y. Han, H. Shen, B.I. Carr, P. Wipf, J.S. Lazo, S.S. Pan, *J. Pharmacol. Exp. Therapeut.* 309 (2004) 64–70.
- [21] J. Sun, Y. Dou, H. Ding, R. Yang, Q. Sun, Q. Xiao, *Mar. Drugs* 10 (2012) 881–889.